Faculty of Science
University of Helsinki

Thermosensitive poly(*N*-acryloyl glycinamide) microgels and their application in catalysis

Dong Yang

DOCTORAL DISSERTATION

To be presented for public discussion with the permission of the Faculty of Science of the University of Helsinki, for public criticism in Auditorium A129 of the Department of Chemistry, on the 22th of October, 2021 at 12 o'clock.

Helsinki 2021

Supervisors

Doc. Sami Hietala
Department of Chemistry
University of Helsinki
Finland

Prof. Heikki Tenhu
Department of Chemistry
University of Helsinki
Finland

Opponent

Prof. Maria Vamvakaki
Department of Materials Science and Technology
University of Crete
Greece

Reviewers

Prof. Carl-Erik Wilén
Laboratory of Polymer Technology
Faculty of Science and Engineering
Åbo Akademi University
Finland

Doc. Juha Heiskanen
Research Unit of Sustainable Chemistry
Faculty of Technology
University of Oulu
Finland

The Faculty of Science uses the Urkund system (plagiarism recognition) to examine all doctoral dissertations.

ISBN 978-951-51-7617-2 (pbk.)
ISBN 978-951-51-7618-9 (PDF)

Unigrafia
Helsinki 2014

Thermosensitive poly(*N*-acryloyl glycinamide) microgels and their application in catalysis

Abstract

Poly(N-acryloyl glycinamide) (PNAGA) is a non-ionic polymer possessing an upper critical solution temperature (UCST) in water and saline solutions. This thesis explores the synthesis of stimuli-responsive PNAGA microgels and immobilization of catalytically active species inside these.

The synthesis of poly(N-acryloylglycinamide) (PNAGA) microgels was conducted in water by free radical precipitation polymerization below the phase transition temperature of PNAGA in the presence of *N,N'*-methylenebisacrylamide crosslinker. These water dispersed PNAGA microgels show reversible size changes, swelling upon heating and shrinking upon cooling. Using these PNAGA microgels as host for nanocatalysts was carried out by loading silver nanoparticles (AgNPs) via reduction of $AgNO_3$.The thermosensitive behavior of the PNAGA microgels was retained after loading AgNPs, and the catalytic activity of the metal particles in 4-nitrophenol reduction was tested under different conditions. Furthermore, it was shown that the catalytic activity of the AgNP–PNAGA microgels could be switched on and off by changing the temperature and utilizing the thermosensitivity.

To realize biocatalytic microgels, immobilization of an enzyme, β-D-glucosidase, was done by encapsulation of the enzyme during the NAGA precipitation polymerization. Properties of these hybrid microgels were studied varying the enzyme-monomer ratio and the degree of crosslinking. The microgel encapsulated enzymes showed enhanced activity at high pH compared to the native enzymes. Tandem catalysts were then produced by further encapsulation of AgNPs. These were used in cascade reactions involving first enzymatic catalysis followed by AgNP induced reduction.

The catalyst loading efficiency as well as the manipulation of the thermoresponsive properties was performed by copolymerizing methacrylic acid (MAA) with NAGA. The volume phase transition behavior and interactions between NAGA and MAA in the poly(N-acryloyl glycinamide-co-methacrylic acid) [P(NAGA−MAA)] copolymer microgels were studied. AgNPs were immobilized inside the P(NAGA−MAA) microgels using both UV light and chemical reduction. The photoreduction resulted in smaller AgNPs and the amount and size of the AgNPs was observed to depend on the content of MAA. The UV-reduced AgNPs show significantly higher catalytic activity than chemically reduced AgNPs in P(NAGA-MAA) microgels.

Acknowledgements

This work was conducted in the years of 2015-2021 at the Department of Chemistry, University of Helsinki and was funded by the China Scholarship Council (CSC) and University of Helsinki.

I would like to express my greatest appreciation to my supervisors Doc. Sami Hietala and Prof. Heikki Tenhu for all the help you provided. Throughout the years I always received your encouragement and support. Thank you also for your instruction, commenting and polishing of my thesis. Through your dedication, I improved a lot.

My collaborators Milla Viitasuo, Heli Eronen, Dr. Fabian Pooch are gratefully acknowledged. Thank you for your input and support.

I wish to thank Prof. Carl-Eric Wilén and Doc. Juha Heiskanen for examing my thesis and Prof. Maria Vamvakaki for being my opponent.

I am grateful to everyone I met in our lab. Speical thanks to Prof. Sirkka-Liisa Maunu, Seija Lemettinen, Juha Solasaari, Dr. Vladimir Aseyev, Vikram Baddam, Tony Tiainen, Dr. Tina Borke, Prof. Robert Luxenhofer, Dr. Joonas Siirilä, Satu Häkkinen, Dr. Sami-Pekka Hirvonen, Dr. Erno Karjalainen, Dr. Qilu Zhang, Jingwen Xia for their excellent support. Thank you to all my colleagues for creating an active vibe in the group. I will always remember our conference trips, Christmas parties, our futsal games, and many other activities.

Finally, I would like to give my appreciation to my parents and my whole family.

Dong Yang

Helsinki, October, 2021

Contents

List of original publications

(I) Yang, D.; Viitasuo, M.; Pooch, F.; Tenhu, H.; Hietala, S. **Poly(N -Acryloylglycinamide) Microgels as Nanocatalyst Platform.** Polym. Chem. 2018, 9 (4), 517–524. https://doi.org/10.1039/C7PY01950E.

(II) Yang, D.; Tenhu, H.; Hietala, S. **Bicatalytic Poly(N-Acryloyl Glycinamide) Microgels.** Eur. Polym. J. 2020, 133, 109760. https://doi.org/10.1016/j.eurpolymj.2020.109760.

(III) Yang, D.; Eronen, H.; Tenhu, H.; Hietala, S. **Phase Transition Behavior and Catalytic Activity of Poly(N-Acryloylglycinamide-Co-Methacrylic Acid) Microgels.** Langmuir 2021, 37 (8), 2639–2648. https://doi.org/10.1021/acs.langmuir.0c03264.

The author's contribution to the publications

For all publications Dong Yang drafted the research plan and conducted most of the syntheses and characterization. Dong Yang analyzed the data and wrote and finalized the manuscripts together with the coauthors.

Abbreviations

NAGA	N-acryloylglycinamide
PNAGA	Poly(N-acryloyl glycinamide)
BIS	N,N'-Methylenebis(acrylamide)
APS	ammonium persulfate
TEMED	N,N,N',N'-tetramethylethylenediamine
SDS	sodium dodecyl sulfate
AgNP	silver nanoparticle
BG	β-D-glucosidase from almonds
pNGP	p-nitrophenyl β-D-glucopyranoside
MAA	methacrylic acid
PNIPAM	poly(N-isopropyl acrylamide)
P(NAGA-MAA)	poly(N-acryloyl glycinamide-co-methacrylic acid)
AAc	acrylic acid
poly(AAm-co-AN)	poly(acrylamide-co-acrylonitrile)
AN	acrylonitrile
PVCL	poly(N-vinylcaprolactam)
BCPS	sodium 3-(((benzylthio)-carbonothioyl)thio)propane-1-sulfonate
VA-044	2,20-Azobis[2-(2-imidazolin-2-yl)propane]dihydrochloride
DBTC	dibenzyl trithiocarbonate
V-70	2,2'-azobis(4-methoxy-2, 4-dimethyl valeronitrile)
CMDT	cyanomethyl dodecyltrithiocarbonate
PAEMH	poly(2-aminoethylmethacrylate hydrochloride)
EDC	N-3-dimethyl(aminopropyl)-N'-ethylcar-bodiimide
PAEMH	poly(2-aminoethylmethacrylate hydrochloride)
PEG	poly(ethylene glycol)
TREGMDA	triethylene glycol dimethacrylate
EGDMA	ethylene glycol dimethacrylate
k_1	reaction rate constant
k_{app}	apparent reaction rate constant
C_0	concentration at time 0
C_t	concentration at time t
DLS	dynamic light scattering
TEM	transmission electron microscopy
NMR	nuclear magnetic resonance spectroscopy
LCST	lower critical solution temperature
UCST	upper critical solution temperature
DSC	differential scanning calorimetry
T	temperature
T_c	cloud point
VPTT	volume phase transition temperature
VPT	volume phase transition
RAFT	Reversible addition−fragmentation chain-transfer
ATRP	Atom transfer radical polymerization
TGA	Thermal Gravimetric Analysis

1. Introduction

1.1 Thermoresponsive polymers

Stimuli-responsive polymers capable of changing their solubility and conformation rapidly with temperature are called thermoresponsive.[1,2,3,4] In some cases, the change occurs gradually or continuously with temperature and these systems may be called as thermosensitive, though the terminology in the published literature is mixed. In both cases, the conformation of polymers will eventually change from a randomly expanded coil to a collapsed compact globule or vice versa.[5] For most of these polymers the coil-globule transition is reversible with temperature change. Two main types of phase transitions can be distinguished (Scheme 1). Polymers that have a lower critical solution temperature (LCST) are soluble at temperatures below the LCST and insoluble above LCST. On the contrary, upper critical solution temperature (UCST) polymers are phase separated below the UCST and dissolved above UCST. The phase transitions are concentration dependent and the LCST and UCST stand for the lowest or highest temperature where the phase transition takes place. The phase transition behavior of LCST or UCST polymers originates from the interactions between the polymer chain segments and the solvent. When polymer-water interactions change into interactions between the polymer segments the previously soluble polymer self-assembles and/or aggregates, and vice versa.[6,7]

Among the LCST-type polymers, poly(N-isopropyl acrylamide) PNIPAM and its copolymers are the most studied due to their phase transitions in the range of human physiological temperature.[8,9] The phase transition of these polymers can be adjusted to a desired temperature through incorporating hydrophobic or hydrophilic groups, such as an amide, carboxyl, or hydroxyl group.[10] Generally, the introduction of hydrophobic groups would shift the cloud point to lower temperature. However, there are exceptions, such as poly(*N*-isopropyl methacrylamide) (PNIPMAM), that has a higher LCST compared to PNIPAM due to the extra α-methyl group coupled to the main backbone that restricts the flexibility of the entire PNIPMAM chain and thus impedes the collapse of the whole system.[11]

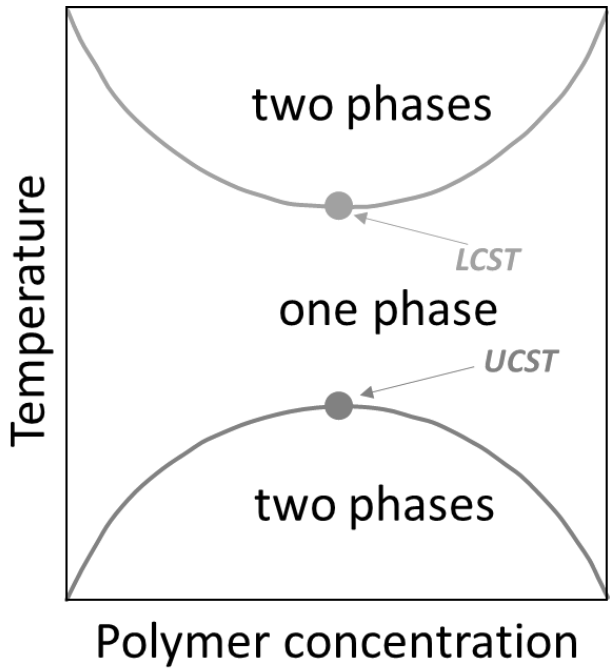

Scheme 1. Idealized phase diagrams of LCST behavior (blue) and UCST behavior (red).

UCST polymers are much less studied than LCST polymers[12] and usually their phase transition is not as sharp as that of LCST polymers, and the transition may change or disappear with a change of conditions. The most studied UCST-type polymers in aqueous systems are poly(sulfobetaine)s,[13,14] poly(acrylamide-*co*-acrylonitrile) (poly(AAm-*co*-AN)),[15,16] poly(N-acryloyl glycinamide) (PNAGA),[17,18] and ureido-derivatized polymers.[19,20] Poly(sulfobetaine)s are zwitterionic polymers based on sulfobetaine monomers. Their UCST-type phase transition behavior stems from the electrostatic interaction between the charged ammonium and sulfonate groups in aqueous solution. The salts screen the charged groups and thus reduce the UCST. Non-ionic poly(AAm-*co*-AN), a copolymer of acrylamide (AAm) and a minor quantity of acrylonitrile (AN) demonstrates UCST that is less sensitive to ionic strength. AN provides hydrophobicity to poly(AAm-*co*-AN) and increasing the content of AN shift the UCST of polymer to a higher temperature. Ureido-derivatized polymers show UCST thermoresponsivity due to the hydrogen bonds between the ureido groups; hydrogen bonding is affected by temperature. Ureido-based UCST polymers possess high stability in salt conditions and the phase transition temperature shows positive dependency to the ureido content. PNAGA is the most studied UCST-type polymer and also with PNAGA a number of factors affect the phase transition, e.g. introduction of ionic groups, molecular weight and molecular weight distribution, addition of electrolytes, and copolymer composition.[21]

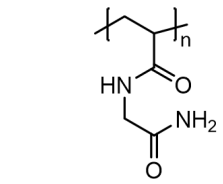

Poly(*N*-acryloyl glycinamide)
PNAGA

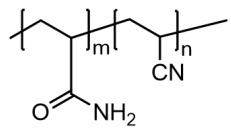

Poly(acrylamide-*co*-acrylonitrile)
Poly(AAm-*co*-AN)

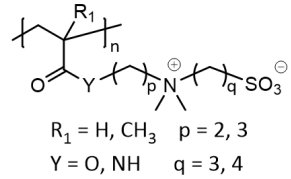

R_1 = H, CH_3 p = 2, 3
Y = O, NH q = 3, 4

Poly(sulfobetaine)

Polymers showing UCST behavior

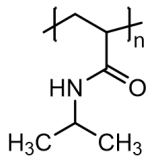

Poly(*N*-isopropyl acrylamide)
PNIPAM

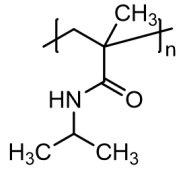

Poly(*N*-isopropyl methacrylamide)
PNIPMAM

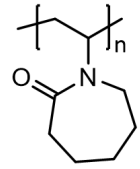

Poly(N-vinylcaprolactam)
PVCL

Polymers showing LCST behavior

Scheme 2. Examples of polymers showing thermoresponse in water

1.2 Polymeric microgels

Polymeric microgels are colloidal gel particles composed of cross-linked polymer chains.[22,23] The term 'microgel' was first given by Baker in 1949 in the study of solvent swellable polybutadiene particles,[24] but majority of the studies on microgels concentrate on aqueous dispersions. As the size of the microgel particles varies from several micrometers down to nanometers, they are sometimes referred to as 'nanogels'.[23] Among the published microgel literature, most of them involve crosslinked poly(N-isopropylacrylamide) (PNIPAM), poly(N-vinylcaprolactam) (PVCL), or their derivatives showing lower critical solution temperature (LCST) behavior.[25–31] In contrast to linear stimuli-responsive polymers, microgel phase transition is often referred to as volume phase transition temperature (VPTT).

The crosslinked microgels with structural integrity are distinctly different from rigid nanoparticles, flexible macromolecules, micelles, or vesicles.[32] Instead of dissolving in aqueous solution, the cross-linked hydrogel particles form a dispersion. In the dispersion, the solvent permeates the particles and causes their swelling. In the swollen state, solvent molecules are able to move inside the particle with high mobility accompanied by the movement of the internal chain segments. The surface of particles

presents itself as an open porous structure, which facilitates the extensive exchange between the interior and the surroundings of the particles. The size and structure of microgel particles are affected by the cross-linking density and the degree of swelling.[33] The swelling degree of a cross-linking polymer colloid depends on the local cross-linking density, and the charge density of ionic groups, but also on the environmental conditions surrounding it. The environmental parameters affecting the swelling behavior of stimuli-responsive microgels are for instance pH, ionic strength, chemical nature of the counterions, and temperature.[33]

Microgels as macromolecular networks have unique properties, such as high molecular weight, low viscosity for their size, and high number of functional groups, allowing them for further functionalization.[34,35] Colloidal stability is another characteristic of aqueous nanogel/microgel particles. The stability of colloidal particles is determined by the combined effects of van der Waals forces and steric or electrostatic forces. In a swollen state, the effect of van der Waals attraction is marginal and the dispersion system is inherently stable. While the system contracts, the Hamaker constant increases resulting in noticeable increase of van der Waals forces and the tendency of colloid aggregation.[36] In microgel synthesis, surfactants are commonly used to improve the colloidal stabilization. These surfactants attach to the surface of particles, impeding the particle aggregations by electrostatic repulsion and steric hindrance.[37] . One of the most often used surfactants is sodium dodecyl sulfate (SDS).[33] Utilizing redox initiators in polymerization or the dissociation/protonation of functional groups (e.g. -OH, -COOH, $-NH_2$), charged groups can be introduced into the particles and scattered on the surface and/or the interior. Due to the strong electrostatic attraction, counterions are absorbed onto the surface building an electric double layer (the Stern layer). The electrostatic field provided by the Stern layer will create a significant electrostatic repulsion between two approaching particles to prevent the contact. Increasing electrolyte concentration will diminish the electrostatic interactions. Zeta potential, ζ , is used to describe the magnitude of electrostatic effect and as an indicator of the stability of dispersion systems.

The thermo-responsive microgels show volume phase transitions, during which they undergo either an abrupt or a continuous change in the degree of swelling. The volume phase transition stems from phase separation of each polymer chain segment within the microgel network upon temperature change.[38,39] A broad transition temperature is often observed for microgels implying a heterogeneous structure inside (e.g. different chain lengths, branching, crystallinity).[40] Microgels exhibiting LCST-type volume phase transition shrink above the VPTT. This property of changing volume upon

temperature has versatile applications including controlled drug delivery, [41,42] membrane separation,[43,44] flow control,[45,46] catalysis,[47–49] and bio-sensing, protein separations[50] or biomedical research! [26,51,52,53]

1.2.1 Synthetic approaches

Microgels can be prepared through polymerization reactions as well as cross-linking of preformed macromolecules.[33]

1.2.1.1 Polymerization reactions

Precipitation polymerization[36,54] and inverse mini- and microemulsion polymerization[55,56] are the heterophase polymerization techniques frequently utilized for microgel synthesis. The polymerization conditions are set so that the phase separation, or volume phase transition (VPT), of the chains take place, leading to precipitation. Nucleation is the first stage in the formation of microgel in precipitation polymerization. After initiator splits into free radicals, the polymerization gets started by radical propagation and chain growth (Scheme 3). At a critical chain length, the oligomeric growing chains begin to collapse at the polymerization temperature below/above VPT. The compact collapsed growing chain forms the nucleus on which the microgel builds up. The nucleus continues growing into larger and colloidally stable polymer particles by aggregating other nuclei or incorporating free monomers. In the presence of a cross-linker, covalently crosslinked particles are formed. Dialysis, centrifugation, and redispersion are the methods used for microgel purification. Precipitation polymerization has been extensively applied for the preparation of thermosensitive PNIPAM[57–59] and poly(N-vinylcaprolactam) (PVCL) microgels.[60–62]

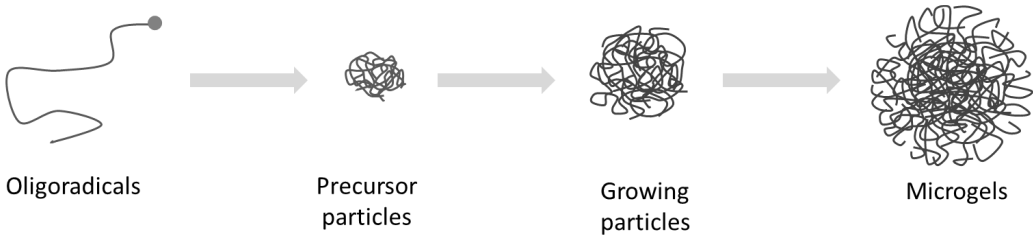

Scheme 3. Illustration of the microgel formation by precipitation polymerization for a LCST-type polymer. The temperature is above the VPTT.

The cross-linker plays a significant role in microgel synthesis. In general, the swelling degree of the

microgels decreases as the concentration of cross-linker increases. The size and swelling properties of the microgels can be varied by using cross-linkers with different solubilities and structures. For instance, the flexibility of the cross-linker may have an effect on the polydispersity and swelling degree of the prepared microgel. Three different cross-linkers, ethylene glycol dimethacrylate (EGDMA), triethylene glycol dimethacrylate (TREGMDA) and N, N'-methylenebis(acrylamide) (BIS) (Scheme 4), were compared in the preparation of PNIPAM microgels.[63] Sizes and the swelling degrees of the microgels were observed to decrease in the sequence TREGMDA-, EGDMA-, and BIS-cross-linked microgels as the space between two directly connected crosslinking points became shorter and the whole cross-linker chain stiffened. [63] The reactivity of the crosslinker compared to the main monomer may also have an effect on the structure of the microgels. For example in the case of PNIPAM, it has been observed that the BIS crosslinker reacts faster than NIPAM, and this leads to microgels with more crosslinked core than the shell.

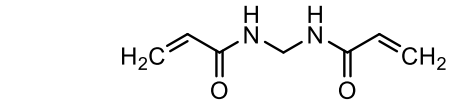

N, N'-methylenebis(acrylamide)
BIS

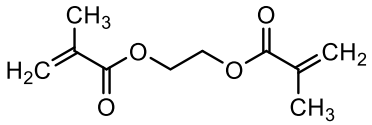

ethylene glycol dimethacrylate
EGDMA

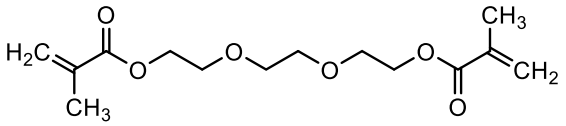

triethylene glycol dimethacrylate
REGMDA

Scheme 4. Structures of crosslinkers: *N,N'*-methylenebis(acrylamide) (BIS) and ethylene glycol dimethacrylate (EGDMA) and triethylene glycol dimethacrylate (REGMDA).

The use of surfactant has an effect on the morphology of the microgel in precipitation polymerization. In surfactant-free system, the stirring rate may have influence on the size of microgels, e.g. higher stirring rate resulted in smaller microgel particles when polymerizing NIPAM.[64]

In the early stage of the microgel formation, the nucleus particles are very small. The charges on the surfaces of the nucleus particles from the incorporated ionic initiator residues are not sufficient enough to prevent nucleus aggregation, this leading to bigger particles. A surfactant needs to be introduced in the microgel synthesis to regulate the size of microgel particles. In the presence of a surfactant, the interfacial tension of nucleus reduces and the hydrated surfactant covering the nucleus forms a sterically stabilizing layer. As a result, the early nucleus aggregation is suppressed and microgels with regulated size and narrow distribution are obtained.

Another way to stabilize the microgel is to involve reactive functional comonomers in the synthesis process. The covalently bound comonomers can bring functional groups into microgels, enhancing the stability and limiting the microgel aggregation. The incorporation of ionic monomers can change the microgels response to pH, electrolyte, and temperature. The high hydrophilicity of ionic comonomer increases the swelling ratio and osmotic pressure while the introduction of hydrophobic comonomer into the microgel may decrease the initial and final microgel radii. For instance, in microgels functionalized with acrylic acid the phase transitions can be modulated by pH due to the (de)protonation of carboxylic groups. PEG macromonomer can be applied to prepare colloidally stable microgels. The content of PEG macromonomer or the length of the PEG chain determines the microgel size. The incorporation of the PEG macromonomers into the microgel structure decreases the swelling degree and induces a shift of the volume phase transition to higher temperatures.[65]

Copolymer microgels are often chemically and topologically heterogeneous. During the polymerization, the comonomer with higher reactivity will be consumed faster leading to a core and a shell with different chemical structures and densities. In the case of aqueous microgels, the more hydrophobic component tends to concentrate in the core during the polymerization process. The increase of hydrophobic content decreases the microgel size. Varying the polymerization process can be used to design specific microgel architectures.[33] Microgels with desired core and shell components can be prepared by sequentially adding different feed solutions. Hollow nanogels can be prepared by selectively dissolving the core encapsulated in hybrid microgels by seeded polymerization.

A variety of emulsion polymerizations (e.g. micro- and miniemulsion, inverse micro- and miniemulsion) can also be utilized for the preparation of extremely small microgels.[66–68] In emulsion polymerization, the reaction loci are stabilized by surfactants and the sizes of final microgels are affected by surfactant concentration. Controlled radical polymerization techniques (e.g. RAFT, ATRP) are also explored in inverse miniemulsion polymerization for the preparation of colloidal

particles of special interest.[69,70]

1.2.1.2 Cross-linking of macromolecules

Microgels may also be prepared by crosslinking the polymers after the synthesis. The cross-linking can be done either by introducing covalent linkages by chemical cross-linking or by reversible connections by physical cross-linking.

Chemical crosslinking

Chemical crosslinking relies on covalent connections between the polymers.[33,71–73] Commonly used chemical reactions for cross-linking are disulfide formation, Michael addition, and condensation reactions.[33,74–76]

Currently, polysaccharides are the biopolymers mostly chosen for microgel preparation, as they demonstrate good biocompatibility, low toxicity.[33] Furthermore, functional groups such as hydroxyl, amino, carboxylic functionalities exist on saccharide units, providing binding sites for the conjunction of other functional compounds, e.g. cross-linking groups.

A variety of polysaccharide-based microgels have been synthesized by the formation of disulfide bonds. To achieve this, it is essential to thiolate the polysaccharide building blocks prior to the microgel synthesis. Multiple methods have been explored for thiolation. For instance, chitosan was thiolated via an amidine bond formed between 2-iminothiolane and amine,[77–79] by coupling N-acetylcysteine through carbodiimide reaction[80], and crosslinked by chloramine-T-mediated disulfide formation[81] (Scheme 5). Disulfide-cross-linking applied to other polysaccharides, e.g. hyaluronan[55,82] and heparin[83] are reported as well.

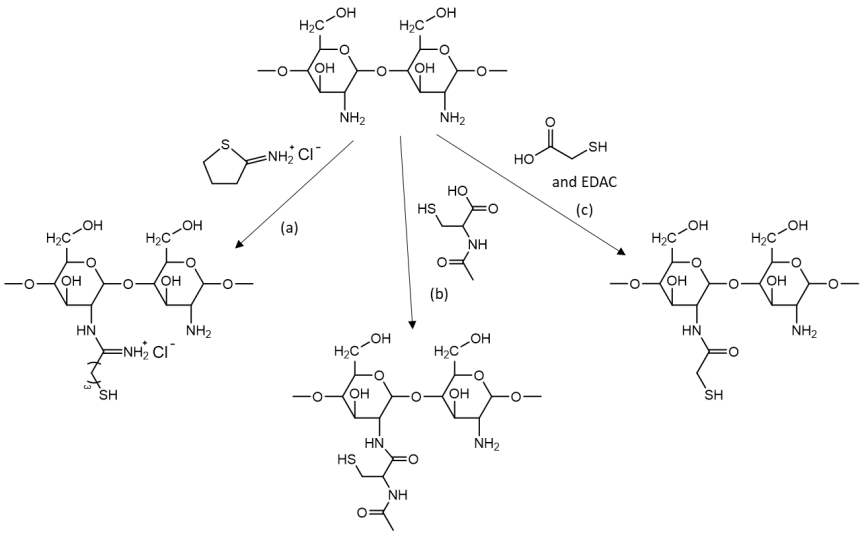

Scheme 5. Synthetic pathway for the modificaiton of chitosan with 2-iminothiolane (a), *N*-acetylcysteine (b), and thioglycolic acid mediated by a carbodiimide (1-ethyl-3-(3-dimethylaminopropyl)carbodiimide hydrochloride; EDAC) (c).

Michael addition is a method commonly used for cross-linking. In Michael addition, a carbanion or a thiol group associates with an α,β-unsaturated carbonyl compound in the presence of bases. Elbert al. et[84,85] prepared microgels with ~100nm average diameter by crosslinking bovine serum albumin (BSA) with eight arm poly(ethylene glycol)-octavinylsulfone (PEG-OVS, MW 10 000). The crosslinking was based on a Michael-type addition between double bonds of PEG-OVS and amines of BSA. Subsequently, the BSA-PEG-OVS microgels were dip-coated onto the surface of thiol-functionalized glass slide through thiol-Michael addition. Thiol-Michael addition is more active than Michael addition based on primary amines. This was utilized in rapid coating before bulk gelation[85] and the microgel-coated glass exhibited reduced protein adsorption and cell adhesion. Sahiner et al. explored a facile one-step method to prepare poly(laminarin) (p(LAM)) microgels crosslinked by divinyl sulfone mediated Oxa-Michael addition reaction. The prepared p(LAM) microgels were spheres with diameters in the range of 0.3-10 μm. They further modified the microgels with chlorosulfonic acid (CSA), a sulfation agent for antitumor activity enhancement, conferring the microgel with excellent blood compatibility and a potential platform for drug delivery.[86]

Condensation reactions, such as glutaraldehyde or carboxylic acid coupling with primary amine, have been utilized in microgel cross-linking. Multiple methods have been explored for the preparation of chitosan particles using glutaraldehyde as a potent cross-linker, e.g. reverse micellar method,

nanoreactors, inverse miniemulsions. Furthermore, a membrane filtration method is a good option to obtain particles with high monodispersity. The diameter of particles can be controlled by the pore size on the membrane. Chitosan particles have been tested as carriers of various drugs and proteins.[80]

Physical crosslinking

Microgels with adjustable mechanical strength can be obtained by chemical cross-linking.[33] However, the utilization of crosslinking agents in chemical cross-linking may cause damage to the integrity of encapsulated bio-substrates (e.g. proteins, cells) and introduce toxic compounds to the microgel networks limiting their applications and increasing the cost.[71] Physical cross-linking can result in networks without using crosslinking agents. Multi inter/intramolecular interactions can drive the formation of physical cross-links and the microgel particles. The main interactions are discussed below.

(i) Electrostatic attraction. Microgels can be prepared by the interaction between the incorporated cationic and anionic functional groups. For example Pelton *et al.*[87] prepared aminophenylboronic acid (PBA)-functionalized amphoteric microgels utilizing acrylic acid (AA) as the anionic monomer and *N,N*-dimethylaminoethylacrylate (DMAEA) as the cationic monomer in the presence of a mixed anionic initiator/cationic surfactant system (APS-CTAB). The colloidal networks of amphoteric microgels were constructed via electrostatic interactions between DMAEA-containing polymer and the microgel precursor. Phenylboronic acid functional groups were grafted onto the microgels in the presence of EDC. The prepared PBA-functionalized microgels exhibited relatively high colloidal stability and interesting glucose-response under physiological conditions.[87]

(ii) Hydrophobic interactions. Amphiphilic block and graft copolymers can assemble into micelles or nanoparticles driven by hydrophobic interactions above the critical micelle concentration (CMC). Amphiphilic block copolymer micelles mostly comprise a hydrophobic core and a hydrophilic shell in aqueous dispersions. The spherical micelles can be 'core-corona' type or 'crew-cut' type depending on the relative lengths of the blocks. Amphiphilic copolymers with long hydrophobic blocks tend to form 'crew-cut' micelles, while extensive hydrophilic blocks contribute to the formation of 'core-corona' micelles. By addition of hydrophobic small molecules, the amphiphilic block copolymer micelles will rearrange to bigger nanoparticles. Overall, the morphology of nanoparticles can be controlled by the molar mass of the amphiphilic block copolymers, the lengths of the hydrophobic blocks, and the chemical nature of the repeating units.[71,88,89]

(iii) Hydrogen-bonding. Aqueous microgels based on hydrogen bonding are rarely reported since water competes with hydrogen bond donors/acceptors in microgel system. Li and Pich[90] reported

redox-active and pH-sensitive chitosan-poly(hydroquinone) microgels synthesized in W/O miniemulsion. The chains were crosslinked with hydrogen bonds between poly(hydroquinone) and chitosan. The microgels crosslinked with hydrogen bonds are biodegradable in aqueous solutions either in the presence of hydrogen bond disrupting agents as urea, or lysozyme, which enzymatically cleaves glucosidic linkages between D-glucosamine/N-acetyl-D-glucosamine units. The controlled and sustained release of a therapeutic drug was investigated by encapsulating an anticancer drug, doxorubicin, and the subsequent release in the presence of the enzyme. The results indicate these microgels can be designed as a matrices for drug carriers navigating to tumor cells.[90]

1.2.2 Application of microgels

The internal cross-linked structure, on one hand, maintains the physical dimensions of the microgel particles and on the other hand allows to use the interior for further applications. Microgels have therefore been used as carriers for drugs, cosmetics or other activates.[8,26,35,41,51,60] These activates can be incorporated through physical entrapment, covalent conjugation, hydrogen bonding, electrostatic or hydrophobic interactions. Microgels with different characteristics (e.g. particle sizes, shell thickness, biodegradability) can be tailored accordingly. The release of the activates is an important aspect and the stimuli-responsiveness brings in multiple possibilities for the controlled release. Additionally, the properties of microgels can be customized with regard to biocompatibility, microporosity, and capability of drug loading. Owing to the porous structure, the microgels have mechanical properties similar to many soft tissues.[33] Recent *in vitro* studies including cellular proliferation within microgel, controlled loading and release of bioactive factors were carried out to establish the introductory groundwork for the further application of microgels on the tissue recovery *in vivo*.[91]

Metallic NPs have drawn much attention because of their catalytic activity.[92–94] However, metal particles in the nanoscale possess high surface energy and tend to aggregate, losing the catalytic activity. The immobilization of metallic NPs onto microgels provides a promising solution on this problem for many reasons. Firstly, the internal cross-linked structure hinders the mobility of metallic NPs, thus enhances their stability. Secondly, microgels with unique architectures and sizes can be easily obtained. The catalytic activity of immobilized metal NPs can be modulated through the microgel responding to the environmental stimuli.

Yan et al.[95] used poly(styrene)-poly(*N*-isopropylacrylamide) (PS-NIPAM) core-shell particles as thermosensitive carriers for AgNP catalysts. The AgNPs were embedded in the crosslinked PNIPAM shell. The reduction of 4-nitrophenol to 4-aminophenol catalyzed by the incorporated AgNPs in the presence of $NaBH_4$ was studied at different temperatures. It was discovered that the catalytic activity slightly decreased after increasing temperature above 25 °C due to the shrinkage of PNIPAM shell that restricted the diffusion of the reactants to catalytically active sites. The shrinkage is related to the cross-linking density of the shell. High cross-linking density decreases the swelling degree of the PNIPAM network alleviating the effect of thermodynamic transition of the microgel shell on the catalytic rate constant.[95]

Amphiphilic, thermosensitive, and polyelectrolyte microgels[92,96–98] have been used to stabilize metal NPs, e.g. Ag@P(NIPAM-co-AAc), Au@PS-NIPAM, Pt@PS-NIPAM, Au-Pt@PS-AEMH. These were used for the oxidation of alcohols to the corresponding aldehydes or ketones in aqueous solutions under aerobic conditions. The microgel-metal nanocomposites exhibited extended catalyst lifetime and resumed their catalytic activity after the reactions.[33]

Enzymatic reactions exhibit high catalytic activity and selectivity at ambient temperature under atmospheric pressure and physiological pH and can be utilized to create more environmentally friendly, cost-effective and sustainable processes.[99–102] Therefore, enzymes have been widely utilized for example in food, pharmaceutical and cosmetics industry. However, enzymes may sometimes be inactivated limiting their application. The immobilization of enzymes with polymeric carriers have emerged as a promising solution to address this. The immobilized enzymes demonstrate not only an improved long-term activity but can also be recovered from the reaction medium. Methods to immobilize enzymes include covalent binding to a carrier and physical entrapment or encapsulation.[102] The covalent binding of enzymes often involves modification of the enzyme to allow the binding to a carrier. This improves their stability but may compromise their activity. The same applies to cross-linking several enzymes into a cluster, which offers highly concentrated enzyme activity in the catalyst, but the covalent conjugation may change the conformation of enzymes. Physical encapsulation of enzymes into microgels avoids those defects since it enhances the enzyme stability and does not harm the native conformation. In 2006, Yan et al.[103] reported for the first time a two-step procedure to encapsulate a single enzyme horseradish peroxidase (HRP) inside a nanogel. These two steps include premodification of the enzyme surface by acryloylation and subsequential in situ aqueous polymerization with acrylamide as the monomer. The encapsulated HRP exhibits

significantly improved stability at high temperature and great tolerance to polar organic solvent. Regarding catalysis, the HRP nanogels revealed very similar catalytic activity to the free HRP. Beloqui et al.[104] simplified the earlier two-step protocols and established a one-step synthesis of single-enzyme nanogels using acrylamide as monomer and sucrose as stabilizer without the premodification of the enzyme surface of glucose oxidase (GOx) by acryloylation. The acrylamide-shelled GOx nanogel demonstrated a broader pH range of optimal enzyme performance. The same experimental setup has been successfully applied to a range of enzymes, e.g. esterase, β-glucosidase, lipase and bovine serum albumin.

1.3 Poly(N-acryloyl glycinamide) (PNAGA)

1.3.1 General properties

Poly(N-acryloyl glycinamide) (PNAGA) is a non-ionic homopolymer showing UCST behavior in pure water as well as in electrolyte solutions. The thermoreversible gelation of concentrated PNAGA solutions was first reported by Haas and Schuler in 1964.[105] The gel formation is based on randomly distributed hydrogen bonds between the repeating units. Breaking of the aggregates can be accomplished not only by temperature but also by hydrogen bond interrupting agents, such as thiocyanate and urea.[106] Also ionic groups unintentionally introduced into PNAGA for example by acrylate impurities in the monomer, cleavage of the amide groups of the side chains, and/or the usage of ionic initiators or chain transfer agents interferes the formation of intra-and/or intermolecular hydrogen bonds. These effects lead to lowering or even disappearance of the phase transition behavior of PNAGA.

1.3.2 Synthesis of poly(N-acryloyl glycinamide) (PNAGA)

PNAGA has been synthesized by free or controlled radical polymerizations.[17,18,107] The first synthesis by Haas and Schular was made by using potassium peroxydisulfate as initiator. Using an ionic initiator leads to the disappearance of the UCST behavior due to the ionic groups from the initiators and acrylate impurities.[108]

Controlled radical polymerization of NAGA by reversible addition-fragmentation chain transfer (RAFT) has been explored using different initiators and chain transfer agents (CTA).[18,108] The introduction of either ionic radical initiators and/or ionic chain transfer agents into the polymer chain

in RAFT polymerization however may suppress the phase transition of PNAGA similarly as was observed in the free radical polymerization. Therefore, using non-ionic radical initiators and non-ionic CTAs for RAFT polymerization of NAGA may guarantee the obtained polymer product with desired molecular masses and uncompromised UCST in water as well as in saline solution.[18] For PNAGA with low molar mass (<20 000), the CTA end group has a strong effect on the cloud point.[17,18] The hydrophobic CTA end group pushes the cloud point of PNAGA to a higher temperature.

Atom transfer radical polymerization (ATRP) can be used for the controlled radical polymerization of NAGA as well.[17] However, the primary amide group in NAGA may complex with copper and disturb the allocation of terminal halogen atoms and thus deactivate ATRP catalyst.[109] Liu et al.[17] synthesized PNAGA with low dispersity in DMSO by using 2-halopropionamide as an initiator and CuX/CuX_2 (X= Cl, Br) with [2-(dimethylamino)ethyl]-amine (Me6TREN) ligand as a catalyst. The polymerization conditions were controlled to avoid the hydrolysis of amide bonds of NAGA. The obtained PNAGA showed an excellent reversibility of UCST-type phase transition in pure water as well as in PBS buffer. The primary amide end-groups introduced from 2-halopropionamide help in eliminating the dependency of the cloud point on molar mass in the low molar mass region.

2. Objectives of the study

This thesis aimed at the synthesis of thermosensitive poly(N-acryloyl glycinamide) (PNAGA) microgels and their characterization. The microgels were prepared by precipitation polymerization and employed as nanocatalyst hosts to improve the stability, activity and control over the catalysis.

In this work:

1. PNAGA microgels with different crosslinking degrees were synthesized by precipitation polymerization. The thermosensitive behavior of PNAGA microgels was studied. Silver nanoparticles (AgNPs) were loaded into the PNAGA microgels by reduction of $AgNO_3$ with $NaBH_4$.
2. Bicatalytic PNAGA microgels were prepared by the encapsulation of an enzyme, β-D-glucosidase, in the PNAGA microgels during the polymerization and subsequent reduction of $AgNO_3$ within PNAGA networks.
3. Poly(N-acryloyl glycinamide-co-methacrylic acid) (P(NAGA-MAA)) copolymer microgels were prepared by copolymerizing NAGA and MAA in the presence of cross-linkers. The phase transition of P(NAGA-MAA) was investigated at different pH. Small AgNPs were

immobilized within the P(NAGA-MAA) microgels by the reduction of $AgNO_3$ under UV light.

4. The catalytic activities of the AgNP-loaded microgels were tested. The enzymatic activity of β-D-glucosidase embedded hybrid microgels was investigated by cleavage of p-nitrophenyl-β-D-glucopyranoside and a cascade reaction was carried out by combining the enzymatic catalysis and reduction of the enzymatic reaction product 4-nitrophenol in the presence of $NaBH_4$.

3. Experimental

The general synthesis and characterizations will be briefly described in this section. More details can be found in the attached publications and their corresponding supporting information.

3.1 Synthesis of hybrid microgels

3.1.1 Synthesis of PNAGA microgels

PNAGA microgels were prepared by free radical precipitation polymerization at 0 ºC in ice bath (Scheme 6). For all syntheses, the total monomer concentration of NAGA and BIS crosslinker was 70mM, APS and TEMED concentrations are 1mM for each and 4mM SDS. Nitrogen was purged into the solution for one hour before the reaction was initiated by adding TEMED and subsequential APS. The reaction was allowed to continue for 6 h, after which the reaction flask was kept at 4 ºC overnight. The resulting product dispersion was purified by extensive dialysis against deionized water.

Scheme 6. Synthesis of PNAGA microgels and Ag-PNAGA hybrid microgels.

3.1.2 Immobilization of AgNPs within PNAGA microgels

The loading of AgNPs inside PNAGA microgels was inspired by the work of Tang et al.[110] First, the PNAGA microgel dispersion (25 ml, 2.8 mg ml^{-1}) were mixed with $AgNO_3$ aqueous solution (10 ml, 0.56 mg ml^{-1}) at room temperature. The mixture was placed in an oil bath at 50 °C and stirred for 24h under a nitrogen atmosphere before it was transferred into a dialysis bag (molecular weight cutoff of 3500 g mol^{-1}) and dialyzed for 2 hours against ice-cold deionized water to remove the free silver ions. The microgel-trapped Ag^+ were then reduced by addition of fresh $NaBH_4$ aqueous solution (10 ml, 0.75 mg ml^{-1}, 19.8mM) into the microgel dispersion in an ice bath. The reaction was left at room temperature for 24 h before it was purified by dialysis against deionized water.

3.1.3 Encapsulation of β-D-glucosidase to PNAGA microgels (BG-PNAGA)

The encapsulation of β-D-glucosidase (BG) by PNAGA was adapted from the synthesis route of polyacrylamide encapsulated enzyme by Beloqui et al.[104] Generally, β-D-glucosidase, NAGA, BIS and sucrose were first dissolved in 5 ml PBS (50 mM, pH = 6.1) in an 8 ml glass vial. The reaction was initiated by the addition of TEMED (4.05 mg, 0.035 mmol) and APS (7.96 mg, 0.035 mmol) after purging with nitrogen for 40 min. The reaction was carried on for 4h before purification by dialysis against deionized water. The end product was collected by lyophilization. The enzyme and crosslinker concentrations were varied.

3.1.4 Immobilization of AgNPs within BG-PNAGA microgels

$AgNO_3$ aqueous solution (5 ml, 0.32 mg ml^{-1}) together with BG-PNAGA dispersion (5 ml, 2.9 mg ml^{-1}) were mixed and kept under stirring while purging with nitrogen for 2h, after which the mixture was dialysed against deionized water to remove the free Ag^+. Fresh $NaBH_4$ aqueous solution (5 ml, 2.42 mg ml^{-1}) was added dropwise into BG-PNAGA(Ag^+) dispersion in ice bath to start the reduction of Ag^+. The reaction was carried on for 4h and then it was purified by dialysis against deionized water for 24 h. The final product was filtered through cotton to remove any possible aggregates before lyophilized.

3.1.5 Synthesis of P(NAGA-MAA) microgels

NAGA and MAA including 3mol% BIS (total concentration: 72mM) was dissolved in 25 ml of deionized water. SDS (4mM) was added and nitrogen was purged for 30min before the reaction was initiated by addition of APS and TEMED. The reaction temperature was adjusted to 16 ºC as MMA has a melting point of 15 ºC. The reactions were carried out overnight followed by dialysis and freeze-drying. Dry microgel powders were purified again to remove the remaining adsorbed TEMED by redispersing in methanol, sonication, centrifugation, and filtration. The washing procedure was repeated three times.

Mixtures of microgel dispersions (1.5 ml; 10 mg ml^{-1} in D_2O) and $AgNO_3$ (1.5 ml; 0.1 M) were exposed to UV light (365 nm) with a nominal 36 W output for 2 h at room temperature. Samples were purified by dialysis against distilled water.

3.2 Characterization

The sizes of the microgels were determined by dynamic light scattering (DLS) either with Malvern Instruments Zetasizer Nano-ZS or with an instrument consisting of Coherent Sapphire 488 nm laser and Brookhaven instruments BI-200SM goniometer, BIC-TurboCorr digital pseudo-cross-correlator and a BIC-CrossCorr detector.

The UV-Vis spectra, transmittance measurements as well as the catalysis studies were performed either with a Shimadzu UV-1601 spectrometer equipped with a circulating thermostated bath, a Jasco J815 CD spectrometer equipped with a Peltier controlled temperature accessory, or a JASCO V750 UV−visible spectrophotometer with a JASCO CTU-100 circulating thermostat unit. All measurements were conducted in quartz cuvettes with a cell path of 10 mm.

^1H NMR spectra of the monomers and microgels were recorded with a 500 MHz Bruker Avance III spectrometer in D_2O. Intensity variations upon temperature change were analyzed by comparing the areas of solvent signal to the polymer signals.

Thermogravimetric analysis (TGA) measurements were performed using Mettler Toledo 850 for Ag-PNAGA microgel samples and NETZSCH Jupiter STA 449 F3 for Ag-P(NAGA-MAA) microgel samples. Samples were placed in a 70 ul Al_2O_3 crucibles and heated from 25 ºC to targeted temperature at a heating rate of 10 K min-1 under nitrogen atmosphere.

Microcalorimetric measurements were performed with Malvern Microcal PEAQ-DSC equipped with

a measuring cell of 0.13 ml. Heating and cooling scans were made at heating rate of 60 ºC/h.

TEM measurements of PNAGA microgel samples were carried out using a Hitachi FESEM S-4800, a FEI Tecnai F20 Field Emission Gun 200 kV or a Jeol JEM-1400 electron microscopes.

4. Results and discussion

4.1 Synthesis of PNAGA microgels

Thermosensitive PNAGA microgels were prepared by free radical precipitation polymerization of NAGA in water at 0ºC in the presence of the BIS crosslinker. The same strategy was extended to in the preparation of PNAGA-coated enzyme microgels and PNAGA copolymer microgels.

Table 1. Microgel properties

	Diameter 20°C [nm]	Diameter 70°C [nm]	Volume change [V(70°C)/V(20°C)]
PNAGA-2%BIS	65	90	2.7
PNAGA-4%BIS	60	96	4.1
PNIPAM-2%BIS	87	78	0.7

The PNAGA microgels with 4 mol% BIS had an average diameter of 60 nm at room temperature and they swelled upon heating, Table 1 and Fig. 8-9. The impact of crosslinker concentration (2, 4 mol%) on the phase transition and the size of the PNAGA microgels is not significant. Using a higher crosslinker concentration, 6 mol%, led to a highly aggregated dispersion. The use of SDS as surfactant was found critical in maintaining the size of microgels, without it particles in micrometer-size with a broad size distribution would be obtained.

Table 2 Enzyme microgel syntheses

Sample[a]	Type	BG:NAGA [molar ratio]	BIS [mol-% NAGA]	BG [m-%]
PNAGA	reference	0:4200	3	
BG-PNAGA4	high enzyme, low xlink	1:4200	3	19
BG-PNAGA10	low enzyme , low xlink	1:10600	3	8.6
BG-PNAGA6	medium enzyme, high xlink	1:6000	16.7	11.5

[a] The sample code refers to excess of NAGA to BG.

BG-PNAGA microgels were prepared by polymerization of N-acryloyl glycinamide in the presence of β-D-glucosidase using sucrose as a stabilizer for the enzyme, Table 2. Full polymerization conversions were reached within 4 h. After the reaction, possible free enzymes and compounds with

low molar mass were removed by dialysis. The enzyme encapsulation was then studied by UV-vis and ^{1}H NMR. In UV, the enzyme containing microgels show a characteristic absorbance peak of β-D-glucosidase at 260nm (Fig. 1 A). However, quantification of enzyme content by UV absorption was not possible due to the scattering by the microgel particles. ^{1}H NMR spectra of BG enzyme, BG-PNAGA physical mixture (molar mass 1:1), PNAGA microgel, and BG-PNAGA microgel were then compared at room temperature (Fig. 1 B). The spectra of BG enzyme and BG-PNAGA physical mixture both show clear signals from the enzyme. However, the signals from enzyme suppress due to the tight encapsulation by PNAGA. DLS analysis of BG-PNAGA microgels shows that the PNAGA encapsulated enzyme microgels have average diameter 100 nm whereas the size of the native enzyme is around 12 nm.

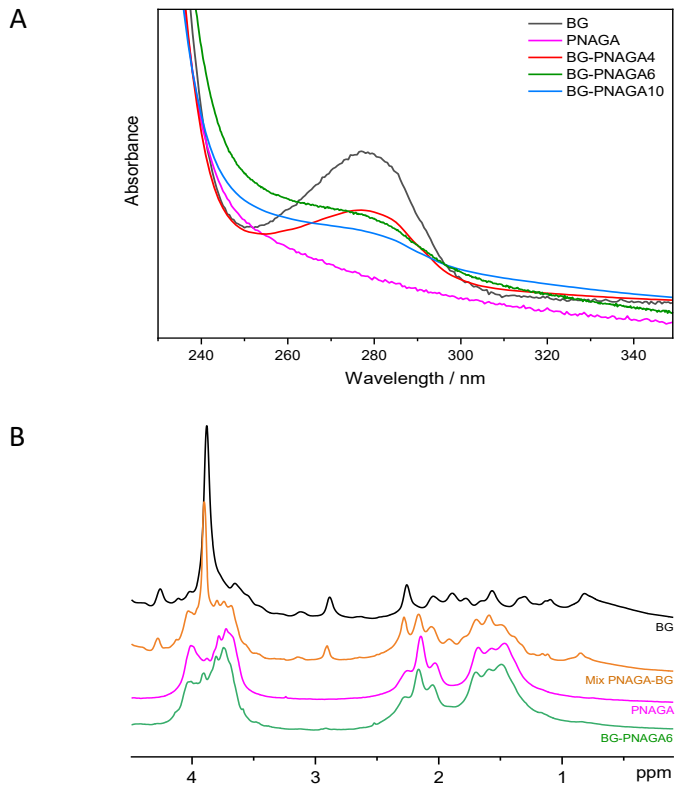

Figure 1 . A) UV spectra of BG, PNAGA, BG-PNAGA4, BG-PNAGA10, BG-PNAGA6; B) 1H NMR spectra of BG, a physical mixture of PNAGA and BG, PNAGA and BG-PNAGA6 at 22 °C.

P(NAGA-MAA) microgels with varying MAA contents were synthesized by free radical precipitation polymerization of NAGA and MAA using APS/TEMED as initiator, BIS as crosslinker,

and SDS as surfactant. The reaction temperature was selected between the expected VPTT of PNAGA and the dissolution temperature of MAA in order to stimulate the precipitation of the initial propagating P(NAGA-MAA) chains. The monomer ratios of the copolymer microgels were calculated using ^{1}H NMR data (Fig. 2 and Table 3). The copolymer compositions were close to the original feed ratios. In order to further confirm the chemical structure of microgels, in situ NMR experiments were conducted using the same reaction parameters as in the microgel synthesis. From the results presented in Fig. 3, NAGA and MAA monomers both were consumed simultaneously in a similar rate for microgel P(NAGA70-MAA30) and P(NAGA50-MAA50), indicating the formation of microgels with likely a random monomer distribution instead of a block or a gradient structure. Similar results have been reported for the copolymerization of NAGA and MAA by RAFT polymerization at 70 ºC.[111] The size of P(NAGA-MAA) microgel at pH 3 was studied by DLS, Table 6. The results show that P(NAGA90-MAA10) and P(NAGA70-MAA30) have hydrodynamic diameters 50 and 57 nm, respectively, at room temperature while the size of P(NAGA50-MAA50) microgel jumps to 240 nm in diameter which can be ascribed to the phase transition-induced aggregation of microgels due to the volume phase transition temperature shifts to lower temperature.

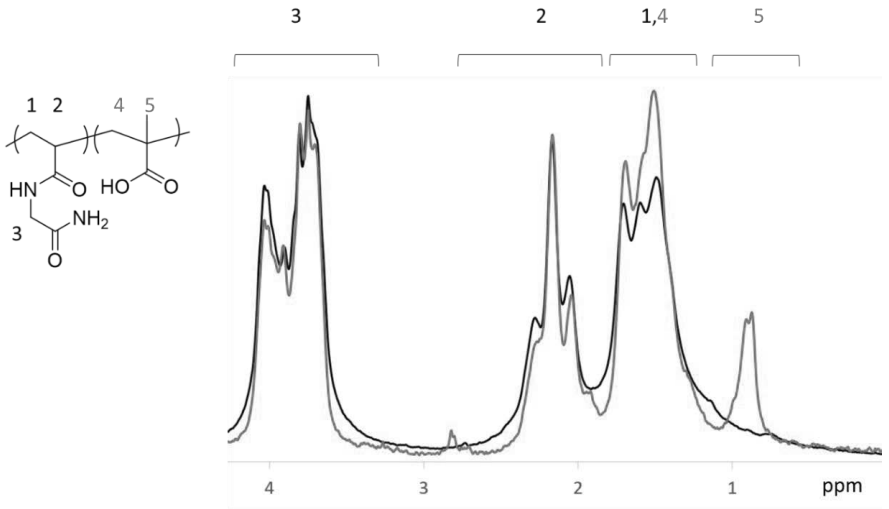

Figure 2. 1H NMR spectra of PNAGA and P(NAGA90-MAA10) microgels at 23 °C.

Table 3. Synthesis of microgels.

Entry	Feed ratio (NAGA:MAA)	Conversion[a] (%)	Copolymer composition[a] (NAGA:MAA)
PNAGA	100:0	87	100:0
P(NAGA90-MAA10)	90:10	79	89:11
P(NAGA70-MAA30)	70:30	83	70:30
P(NAGA50-MAA50)	50:50	67	49:50
P(NAGA30-MAA70)	30:70	75	32:68

[a] by NMR. The copolymer composition was taken as the ratio of NAGA CH_2 signals and MAA methyl group signals

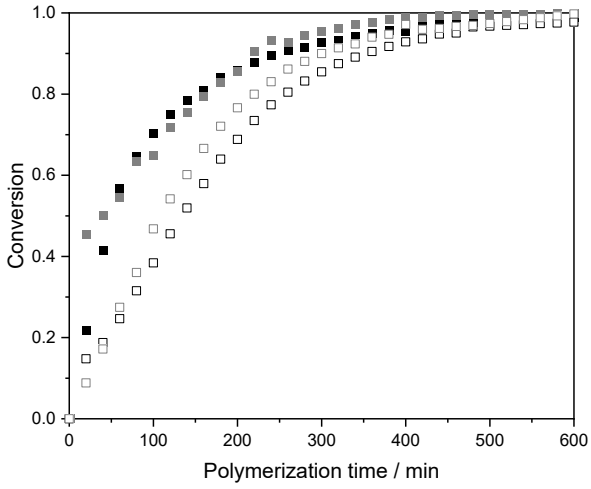

Figure 3. Conversion of P(NAGA70-MAA30) (NAGA ■, MAA ■) and P(NAGA50-MAA50) (NAGA □, MAA□) against reaction time.

4.2 Immobilization of AgNPs on PNAGA microgels

For the synthesis of AgNPs within PNAGA microgels, the microgels were incubated in $AgNO_3$ solution followed by dialysis to remove free Ag^+ ions. Hence, all retained Ag^+ ions were supposedly inside the microgels before addition of fresh $NaBH_4$ aqueous solution into ice-cold PNAGA(Ag^+) microgel dispersion. The dispersions turned instantly yellow indicating the formation of AgNPs. The sizes of PNAGA microgels slightly increased after AgNPs immobilization. Surprisingly, DLS showed that the higher crosslinked Ag-PNAGA-4%BIS had a larger size than Ag-PNAGA-2%BIS. Similar phenomenon had been observed for PS-PNIPAM core-shell particles, where 5% and 10% crosslinker leads to a larger size increase upon AgNPs immobilization compared to 2.5% crosslinker particles.[93] The reason could be the heterogeneous distribution of the crosslinker inside the microgels. The size of PNAGA microgels shown in TEM images conforms the results from DLS (Figs. 4, 8, 9). As can be seen, the AgNPs were located inside the microgels. UV-vis spectra were also used to study the hybrid microgels. The sizes of AgNPs in Ag-PNAGA-2%BIS are larger than those of Ag-PNAGA-4%BIS, as the densely crosslinked structure limits the growth of AgNPs and decreases the silver loading (Table 4).

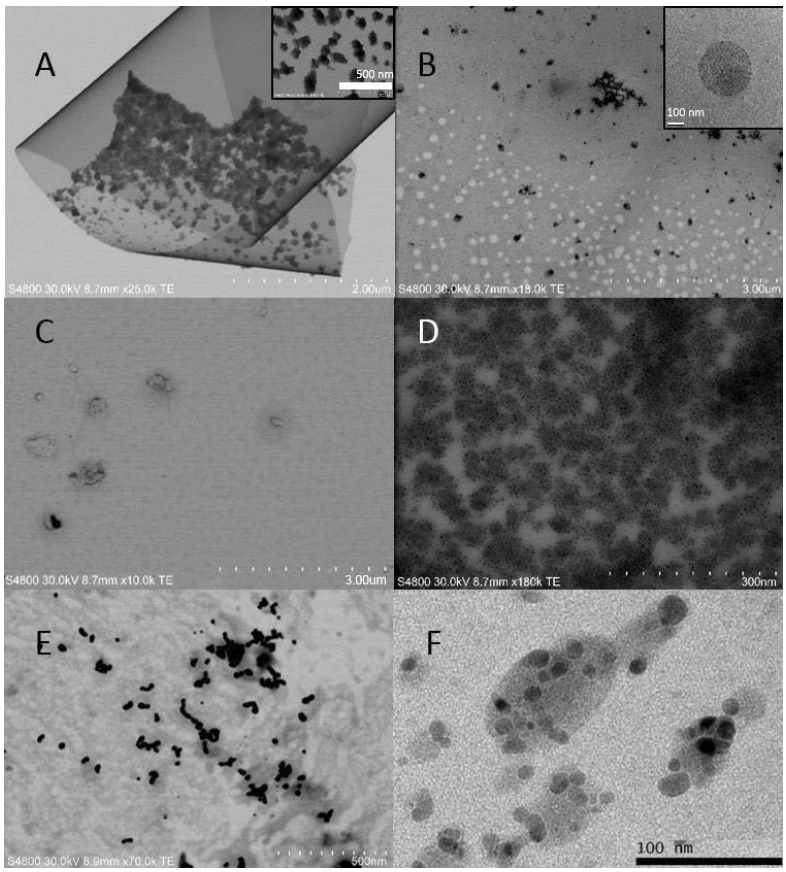

Figure 4. TEM images of A) PNAGA-2%BIS, B) Ag-PNAGA-2%BIS, C) PNAGA-4%BIS, D) Ag-PNAGA-4%BIS, E) AgNP-SDS and F) Ag-PNIPAM-4%BIS.

Table 4 Properties of the AgNP microgels

	AgNP content [a] [wt-%]	**AgNP size [b] [nm]**	**AgNP Surface area[c] [nm^2]**
Ag-PNAGA-2%BIS	12.5	6.2 +/- 1.7	$1.1*10^{19}$
Ag-PNAGA-4%BIS	7.7	4.7 +/- 1.9	$8.1*10^{18}$
Ag-PNIPAM-2%BIS	4.4	8.6 +/- 2.5	$2.7*10^{18}$
AgNP-SDS	0.008[d]	25.1 +/- 7.5	$2.1*10^{19}$

[a] TGA [b] TEM image analysis [c] in 1 g of dry sample [d] Ag content in dispersion, estimated assuming full conversion of $AgNO_3$ to AgNPs

The same method was used to add AgNPs inside BG-PNAGA6 microgels, thus making them capable

for cascade catalysis. TEM results (Fig. 5) show microgel particles with similar size as observed by DLS. For AgNP containing BG-PNAGA6, multiple AgNPs with size varying 5-10 nm were observed inside the microgels. Due to the similar contrast of the enzyme and the PNAGA, the enzymes cannot be distinguished from the surrounding PNAGA network on TEM images.

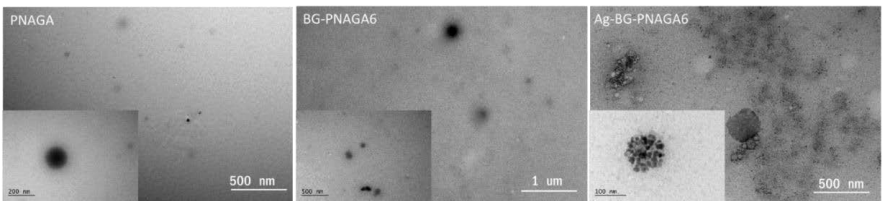

Figure 5. TEM images of PNAGA, BG-PNAGA6 and Ag-BG-PNAGA6

In the case of AgNP-P(NAGA-MAA) microgels, AgNPs were loaded using two methods; either by UV-irradiation or chemical reduction by $NaBH_4$. UV-vis spectrometer was used to monitor the formation of AgNPs by 365 nm irradiation. As can be seen in Fig. 6, the signal intensity of AgNPs increases throughout the irradiation time. But the surface plasmon resonance band of AgNPs centered at ~430 nm for the PNAGA microgels while the band for the P(NAGA70-MAA30) microgels located at 405nm and 505 nm. The constant band at 430nm indicates the formed particles with sizes larger than ca. 2-3 nm.[112] When the UV-reduced silver aggregates into silver clusters, Ag_n^+ (n: 4~9), the absorption peaks at 490-520 nm will be observed.[113] Compared to chemically reduced AgNPs, the UV-reduced AgNPs are smaller and thus have larger surface area. The microgel particles and loaded AgNPs are shown in Figure 7. The Ag content by TGA results, Table 5, demonstrates the higher MAA content leads to a higher overall silver content.

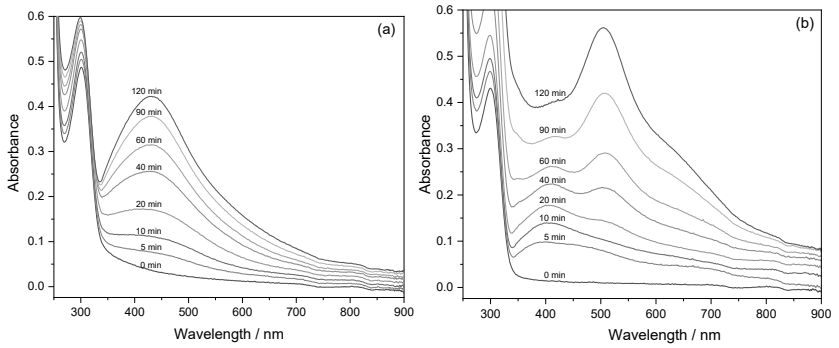

Figure 6. Uv-vis spectra upon irradiation of the (a) PNAGA and (b) P(NAGA70-MAA30) microgels in $AgNO_3$ dispersions.

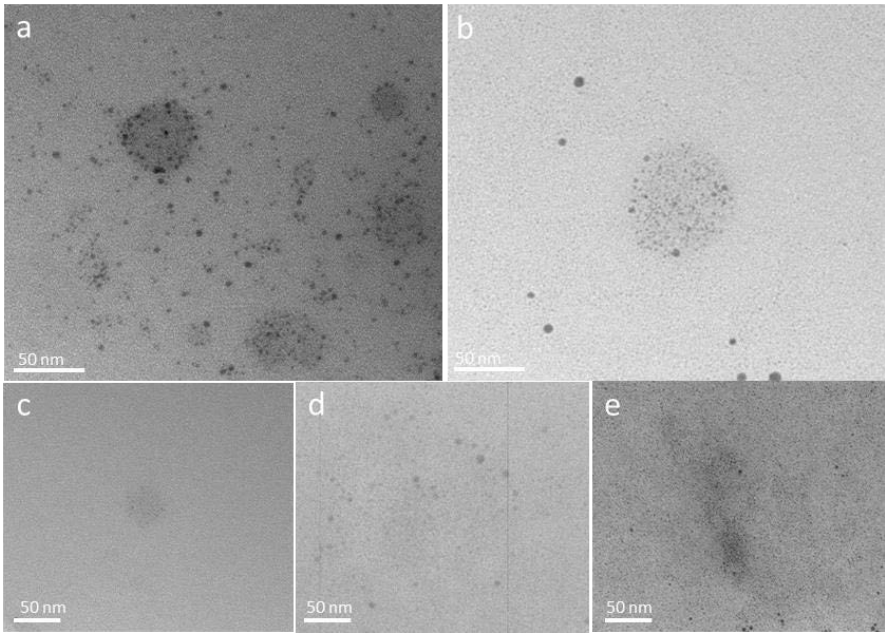

Figure 7. TEM micrographs of silver nanoparticle containing microgels. From left to right: Ag-PNAGA reduced with NaBH4, PNAGA UV, P(NAGA90-MAA10), P(NAGA70-MAA30) and P(NAGA50-MAA50).

Table 5. AgNP content and catalytic efficiency of microgels.

Entry	Ag-content [m-%]	Apparent rate constant [s^{-1}]	Ag mass corrected rate constant [s^{-1} mg^{-1}]
AgNP-PNAGA[a]	8.0	0.91	538
AgNP-PNAGA[b]		1.87	
AgNP-P(NAGA90-MAA10)	15.6	6.94	658
AgNP-P(NAGA70-MAA30)	18.3	20.2	1681
AgNP-P(NAGA50-MAA50)	17.3	23.6	2399

[a] Ag reduced with $NaBH_4$ [b] Ag content could not be determined.

4.3 Thermosensitivity study of PNAGA microgels

Unlike LCST-type polymer microgels that shrink upon heating and swell upon cooling, UCST-type

polymer microgels show opposite phase transition behavior. However, often the phase transitions of UCST polymers are more susceptible to the polymer structure and environmental conditions than the LCST-type transitions. For instance, linear PNAGA shows UCST-type phase transition over a broad temperature range and its UCST-type phase transition varies upon the pH and incorporated ionic groups. This is also the case with PNAGA microgels, as the particle size increases continuously upon heating from 5 ºC to 70 ºC in water (Fig. 8 and Fig. 9). This continuous swelling and shrinking behavior has also been observed for bulk BIS crosslinked PNAGA hydrogels in water and saline solutions.[114] High crosslinking density should restrict the swelling of hydrogel. However, in the case of PNAGA microgels, increasing the crosslinker ratio from 2% to 4% does not change the swelling degree as expected. One possible reason could be that the BIS crosslinker has a higher reactivity than NAGA monomer and leads to a gradient structure from the core to the surface of the microgel particles.[25] Similar effects have been observed on poly(*N*-isopropylmethacrylamide) microgels, where the diameter and swelling degree first decreased with increasing the amount of crosslinkers and increased again upon further increasing the amount of crosslinker. [115]

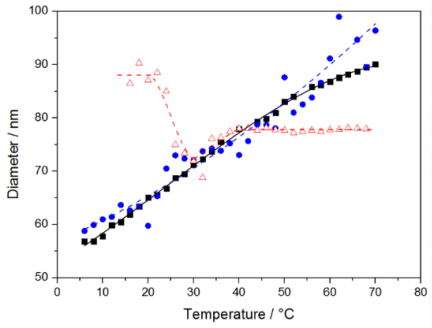

Figure 8. Size of (■) PNAGA-2%BIS (●)PNAGA-4%BIS and (Δ)PNIPAM-2%BIS microgels upon heating based on DLS.

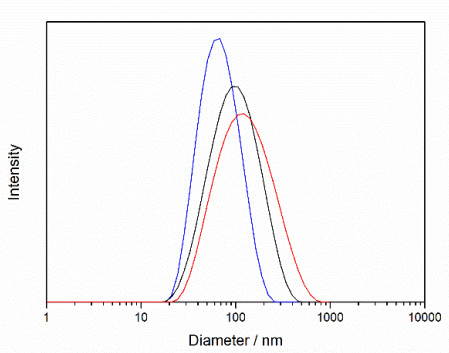

Figure 9. Size distributions from DLS of PNAGA-2%BIS microgel at 10°C (blue), 40°C (black) and 70°C (red)

The phase transition of PNAGA microgels was also studied by variable temperature ^{1}H NMR experiments (Fig. 10). PNAGA microgel shows the strongest signal intensity at 50 ºC and the signal gradually decreases upon cooling until being nearly fully suppressed at 5 ºC. The signal variation is related to the phase transition - at high temperature the hydrogen bonds within microgels dissociate leading to polymer chains with higher mobility and increased NMR signal intensity.

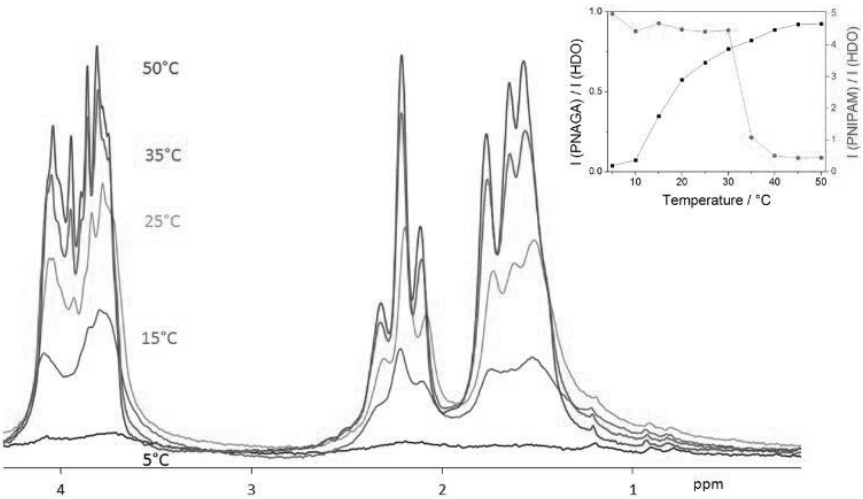

Figure 10. Variable temperature ^{1}H NMR signals of PNAGA-4%BIS microgel in D_2O. Inset: Corresponding integrated signal intensity at different temperatures compared with the solvent (HDO) signal. (■) PNAGA-4%BIS and for comparison (●) PNIPAM-2%BIS.

Unlike the relatively sharp volume phase transition of PNIPAM microgels, PNAGA microgels show gradual changes due to the change of the interactions of the polymer segments within the microgels. The ^{1}H NMR signal intensities of the BG-PNAGA6 microgel increase with heating, proving the microgel with encapsulated enzymes retains the thermosensitivity of PNAGA network.

Thermal behavior of the microgels was studied by differential scanning microcalorimetry (DSC). Upon heating the UCST-type phase transition of PNAGA shows as a broad endothermic transition in the temperature range from 30 to 55 ºC, Fig. 11. The result is different compared to a previous report of DSC measurement for linear, monodisperse PNAGA in water, where the endothermic transition occurs between 5 and 30 ºC. The shift to higher temperature in the case of PNAGA microgels can be ascribed to minute impurities in NAGA monomer, buffer solution used instead of water or to the heterogeneous network structure of the microgels as the phase transition of linear PNAGA relies heavily on these factors as well.[108]

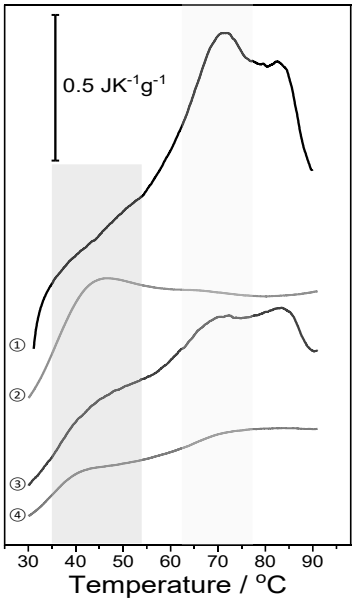

Figure 11. Concentration normalized thermograms of BG and the microgels 1) BG (1 mg/ml) 2) PNAGA microgel (7 mg/ml) (3) mixture of PNAGA microgel and BG (1 mg/ml, mass ratio=1:1) 4) BG-PNAGA6 (6 mg/ml). The highlighted areas are to guide the eye.

Upon heating native β-D-glucosidase denatures and shows a two-step endothermic transitions with maxima at 70 and 85 ºC. Above 85 ºC, the signal deviates heavily from the baseline. We believe the two-step endothermic transition originates from unfolding of different domains in the protein and the signal distortion against the baseline at high temperatures due to aggregation followed by precipitation. When β-D-glucosidase (BG) is mixed with PNAGA microgel, both endothermic transitions are observed at the same temperatures as their individual components. But the endothermic transition of BG unfolding shifts a little to higher temperature indicating possible interaction between the enzyme and the polymer. The BG-PNAGA microgels also show two endothermic transitions corresponding to BG and PNAGA. The phase transition of PNAGA shifts to lower temperature while the unfolding of BG shifts to higher temperature and no baseline distortion is observed at elevated temperature. This demonstrates the capability of PNAGA to act as a stabilizer for enzymes. The phase transition of PNAGA network of BG-PNAGA microgels makes the diameter increase monotonously from ~30 to ~45nm upon heating as observed in DLS. The pure enzyme has a hydrodynamic diameter in native state ~12 nm and there is no change until a sudden increase takes place at 40 ºC due to the aggregation of the denatured enzyme.

P(NAGA-MAA) microgels

In order to study the phase transition behavior of P(NAGA-MAA) microgels, P(NAGA-MAA) samples were dispersed in water at concentration of 10 mg/ml at room temperature, Fig. 12 (top). All P(NAGA-MAA) samples are transparent indicating no large aggregates exist. When samples were cooled to 4°C, PNAGA microgel showed visible clouding while the MAA-containing samples still stayed clear indicating the absence of the phase transition. As said before, minute acrylic acidic impurities in linear PNAGA can suppress its phase transition behavior in water due to the destabilization of the hydrogen bonds. Therefore, charged MAA units affect the interactions between MAA and NAGA repeating units, causing the disappearance of the phase transition behavior near neutral pH. When the pH was lowered to 3, Fig. 12 (bottom), all samples became turbid at 4 ºC, and cleared again at 40 ºC.

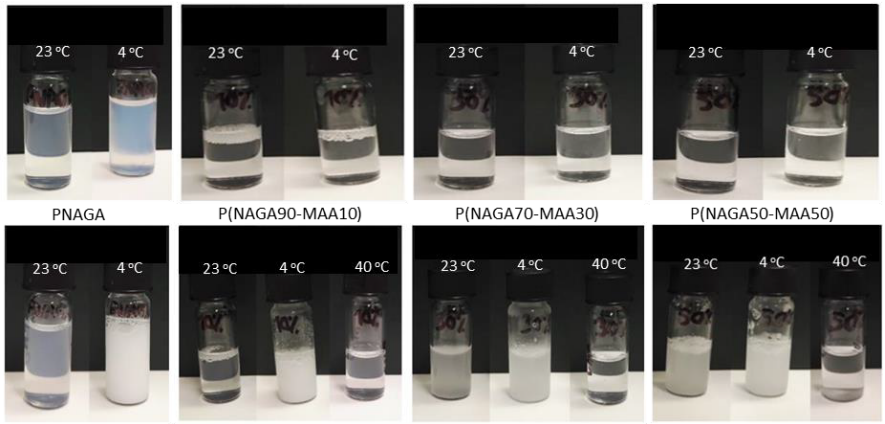

Figure 12. Top row: PNAGA and P(NAGA-MAA) dispersions at different temperatures without adjusting the pH. Bottom row: PNAGA and P(NAGA-MAA) at pH3.

The phase transition behavior was studied by transmittance at pH 3, Fig. 13 and Table 6. The results show a complex temperature dependency. The onset of the phase transition, referred to as the cloud point, Tc, for the PNAGA microgel is at 25°C. The Tc of P(NAGA90-MAA10) shifts to 21 ºC and the Tc of P(NAGA70-MAA30) shifts to 23 ºC. Significant increase occurs with P(NAGA50-MAA50) where the onset is at 36 ºC. At MAA contents below 30 mol%, the phase transition temperature of P(NAGA-MAA) microgel decreases as increasing the amount of MAA while at MAA contents above 30 mol%, the system show opposite tendency. This phenomenon can be interpreted as a combined effect of inter/intramolecular hydrogen bonds between NAGA/MAA and the remaining ionization of the MAA units at a pH close to the pK_a of MAA.[111] At low MAA content, MAA units disturb the formation of hydrogen bonds between NAGA units, yet they are not capable of forming new strong bonds with either NAGA units or themselves. Further increasing MAA content, the interaction

strengthens.

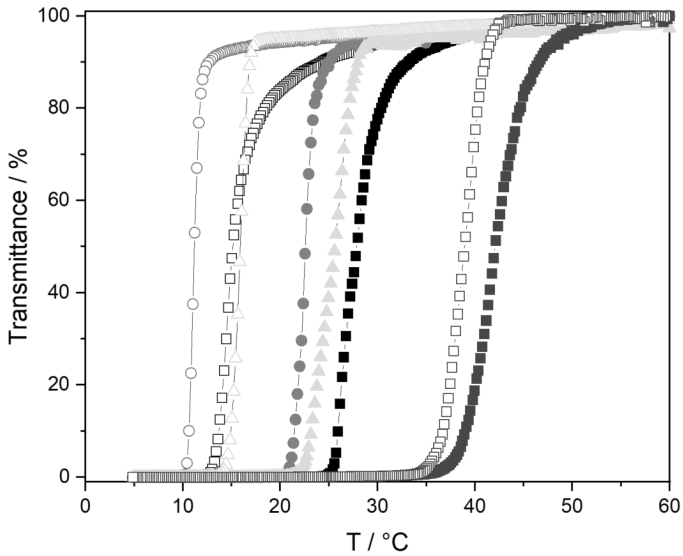

Figure 13. Turbidity curves measured for 10 mg/ml microgel dispersions at pH 3: PNAGA (■,□), P(NAGA90-MAA10) (●,○), P(NAGA70-MAA30) (▲,△) and P(NAGA50-MAA50) (■,□). Closed symbols heating, open cooling.

Table 6. Phase transition behavior of the microgels at pH 3.

Entry	D_h at 15/25/40°C[a] [nm]	Onset heating [°C]	Onset cooling [°C]	Hysteresis [°C]
PNAGA	73 /83 /80[b]	25	15	11
P(NAGA90-MAA10)	44/50/63	21	11	11
P(NAGA70-MAA30)	47/57/80	23	16	9
P(NAGA50-MAA50)	404/240/116	36	38	4

[a] by DLS [b] measured at neutral pH

The thermosensitive behavior of P(NAGA-MAA) microgels in dilute solution was studied also by DLS, Table 6. PNAGA microgels with 10 and 30% MAA swell upon heating similar to PNAGA while the P(NAGA50-MAA50) shrinks, Fig. 14. The continuous change in size indicates non-aggregated microgels undergo a gradual volume change instead of a clear phase transition. At low temperatures, P(NAGA50-MAA50) microgels form much larger particles which first shrink upon

heating and then swell upon further heating after a minimum is reached. This behavior originates from the initial de-aggregation of the particles upon heating and the following swelling of individual microgel particles.

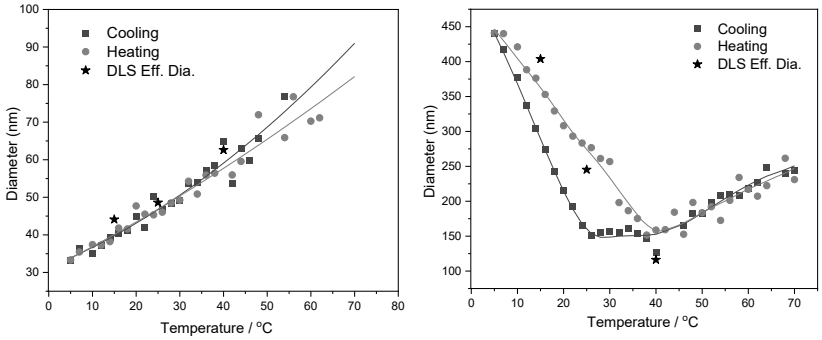

Figure 14. DLS and zetasizer data compared for P(NAGA90-MAA10) left and P(NAGA50-MAA50) right.

The UCST-type thermal behavior of PNAGA microgel originates from hydrogen bonding between the amide groups. The cleavage process of amide-amide hydrogen bonds is an endothermic process while that of amide-water hydrogen bonds gives exothermic signals. DSC results for P(NAGA-MAA) microgel dispersions in water at pH 3 are presented in Fig. 15. Two broad endothermic transitions were observed for PNAGA microgels in acidic conditions at around 5-20 and 30-80 ºC. With the incorporation of MAA into the microgel network, both endothermic signals are suppressed and shifted to a lower temperature. Further increasing the content of MAA leads to a more suppressed endothermic peak. A possible explanation is that the DSC instrument only detects the cleavage of hydrogen bonds between NAGA units. The interaction change between NAGA and MAA units or between the MAA units is not detected by DSC due to the compensation from the formation of new hydrogen bonds or the endothermic transition below the sensitivity of the instrument.

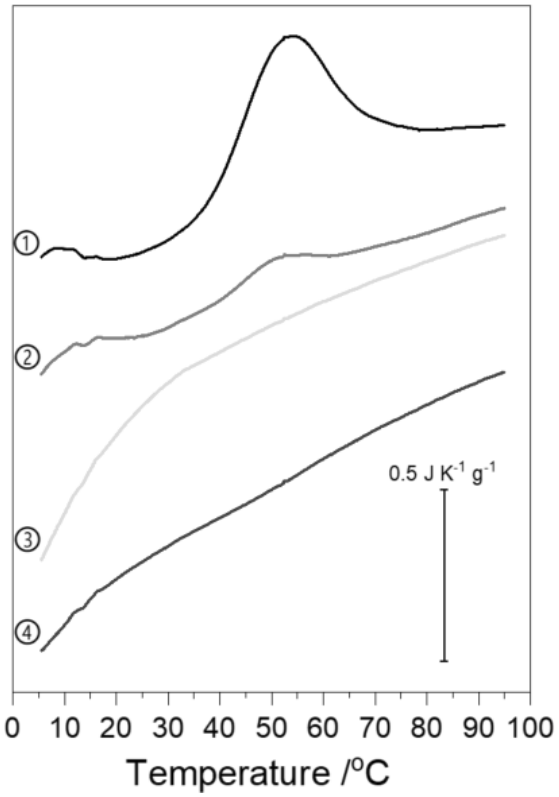

Figure 15. Microcalorimetry scans in water at pH 3. 1. PNAGA 2. P(NAGA90-MAA10) 3. P(NAGA70-MAA30) 4. P(NAGA50-MAA50).

The enthalpies of the thermal transitions of P(NAGA-MAA) microgels can only be considered qualitative due to the baseline. The enthalpies at low temperature are at the same level as the value reported earlier (0.7 J/g)[108] while the endothermic signal at higher temperatures has much higher enthalpy. The reason why several maxima appear remains unknown. One possible reason is the simultaneous endo- and exothermic processes taking place during heating.

When the P(NAGA-MAA) copolymer microgels were studied by variable temperature NMR in D_2O, no intensity changes were observed. At pH 3, signals were suppressed for both NAGA and MAA upon cooling indicating low polymer mobility due to enhanced inter- and intra-polymer interactions. Upon heating, the NMR signals intensify by the same scale regardless of the NAGA-MAA ratio, indicating that the two monomers are simultaneously involved in the phase transition process.

Results from turbidimetry, calorimetry and NMR shows very different the phase transition temperatures. This is because different techniques examine different aspects of the phase transition process. Signals detected by NMR reflect the dynamics of the polymer chains which are determined

by the inter- and intramolecular hydrogen bonding interactions between the NAGA amide groups and uncharged MAA. The endothermic phase transition observed by DSC at 5-15 ºC is in agreement with the drastic change of NMR signal intensity within the same temperature range. At the same time, no turbidity is observed in transmittance measurements indicating that the phase transition processes at low temperature only occur inside the microgels and do not result in the aggregation of microgels. For the endothermic process at higher temperatures, NMR shows unchanged signal for the copolymer microgels upon heating. This indicates that an overall phase transition-induced de-aggregation is ongoing, which is then observed by DLS and DSC. Similar phenomena have been observed for aqueous solutions of hydrophobically modified poly(2-isopropyl-2-oxazolines)[116] and azopyridine-modified PNIPAM[27].

4.4 Catalysis

Ag-PNAGA microgel

The reduction of 4-nitrophenol in the presence of $NaBH_4$ was used as a model reaction to study the catalytic activity of Ag-PNAGA microgels. The reduction kinetics was monitored by UV-vis recording the characteristic absorbance of 4-nitrophenolate at 400 nm at different temperatures, Fig. 16-17. A certain induction time (Fig. 17) was observed at low temperature before the reduction fully began. This is due to the collapsed Ag-PNAGA microgels that slow down the diffusion of reactants inside. Increasing temperature shorten the induction times for all microgels.

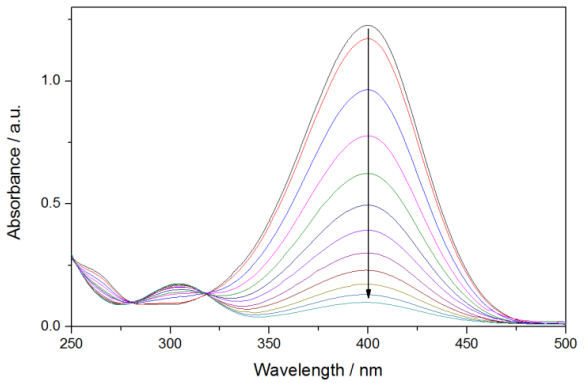

Figure 16. UV-vis spectra of nitrophenol reduction exemplified with insertion of 13 ml of Ag-PNAGA-2%BIS added at 22°C followed from 0 to 33 minutes. (in the direction of arrow, 0 min, 3 min, 6 min, ……33 min)

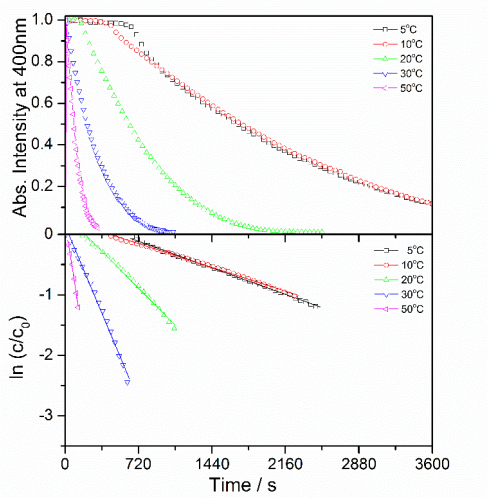

Figure 17. Kinetics of 4-nitrophenol reduction with addition of Ag-PNAGA-4%BIS microgel monitored by UV-vis.

Shortly after the induction time, the reaction obeys pseudo-first order kinetics. By linear fitting the curve of $\ln(c/c_0)$ versus time, the apparent rate constants, k_{app}, can be obtained from the slope. Based on the k_{app} value and the known amount and size of the AgNPs the catalytic activity k_1 can be calculated.

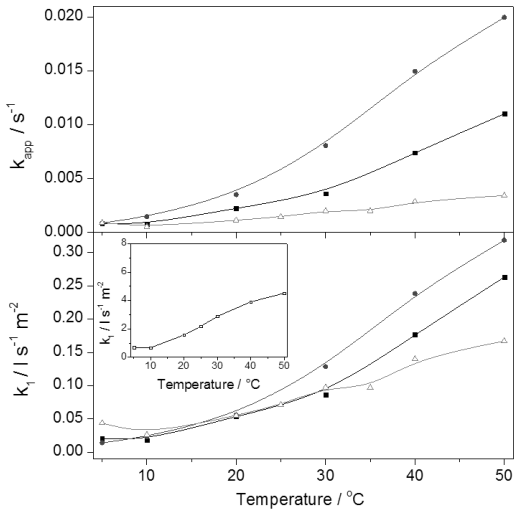

Figure 18. Apparent (k*app*) and normalised rate constants (k_1) of 4-nitrophenol reduction vs. temperature. Symbols (■) Ag-PNAGA-2%BIS (●) Ag-PNAGA-4%BIS and (△) Ag-PNIPAM-2%BIS and inset (□) for AgNP-SDS .

Compared to the reference material, Ag-PNIPAM-2%BIS microgel, Ag-PNAGA microgels have generally higher apparent rate constants, k_{app}, that can be ascribed to the higher AgNP content and smaller AgNP size. Due to the different thermal responses of PNAGA and PNIPAM, Ag-PNAGA microgels have lower reaction rate and longer induction time at low temperatures. The catalytic efficiency of Ag-PNIPAM-2%BIS suppresses slightly at 35 ºC (Fig. 18), nearby the VPTT of PNIPAM. The decrease of catalytic efficiency is due to the shrinking of the LCST-type microgel, which hinders the diffusion of reactants[93,117,118]. At temperature above 30 ºC, the catalytic efficiency of Ag-PNAGA microgels increase significantly due the expansion of PNAGA microgel networks. Because in the Ag-PNAGA-2%BIS the AgNPs are larger than in the Ag-PNAGA-4%BIS, the former has lower k_1.

The thermoreversible swelling behavior of the PNAGA microgel can be employed to tune the catalytic activity by modulating the diffusion through temperature variation. Ag-PNAGA-4%BIS microgel dispersion was added to the 4-nitrophenol solution containing $NaBH_4$ at 50 ºC (Fig. 19). The reduction process began instantaneously as expected. After that, the system was cooled down to 5 ºC for 5min. The reaction almost stopped at 5 ºC due to the contraction of microgels. Increasing temperature back to 50 ºC, the reaction continued. The circle was repeated for 3 times. The obtained result demonstrates that the catalytic activity of Ag-PNAGA microgels can be turned 'on' or 'off' by

temperature variation, which can be further utilized for the design of temperature modulated catalytic processes.

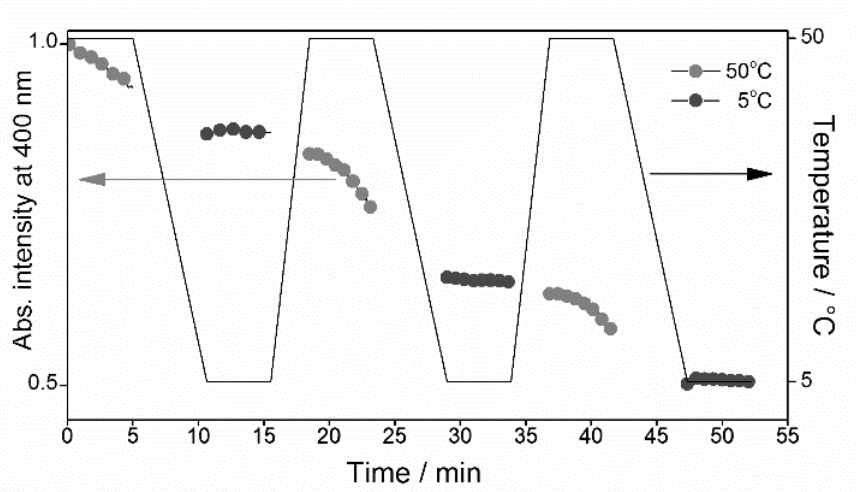

Figure 19. Decrease of 4-nitrophenol absorbance versus time while changing the temperature. Microgel Ag-PNAGA-4%BIS, concentration 0.0149 mg/ml.

Ag-BG-PNAGA microgels

The enzymatic activity of free and immobilized enzymes was explored at different pH by p-nitrophenyl-β-D-glucopyranoside (pNPG) cleavage at 40 ºC, Fig. 20. The optimal pH for the free enzyme is pH 5.6 according to the literature[119] while in our case the optimal pH was found to be at pH 6.1. For the microgel immobilized BGs the optimal pH shifts to at pH 7 but the optimal enzymatic activities are comparable. At high pH, the free enzyme loses its activity quickly, while the immobilized enzymes retain the activity better. The BG-PNAGA6 microgel with the highest crosslinking degree preserves 25% of its optimal activity at pH 10.

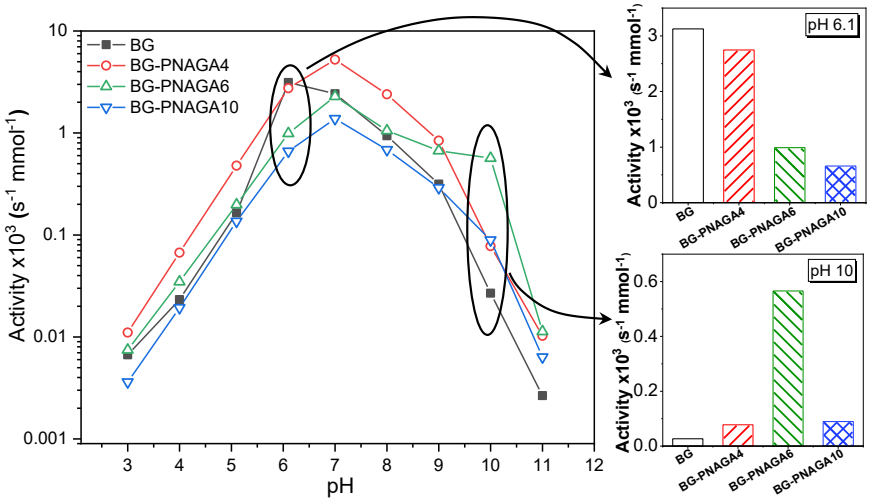

Figure 20. Enzymatic activity at different pH at 40°C.

The cascade catalysis of Ag-BG-PNAGA6 hybrid microgel was studied using two step reaction of pNPG. In the cascade, first an enzymatic pNPG cleavage producing 4-nitrophenol takes place and it is followed by the reduction of 4-nitrophenol to 4-aminophenol by AgNPs in the presence of $NaBH_4$. $NaBH_4$ was added to the reaction at predetermined time. As controls, pure BG and BG-PNAGA6 were tested to rule out the possibility of 4-nitrophenol reduction without AgNPs, Fig. 21A.

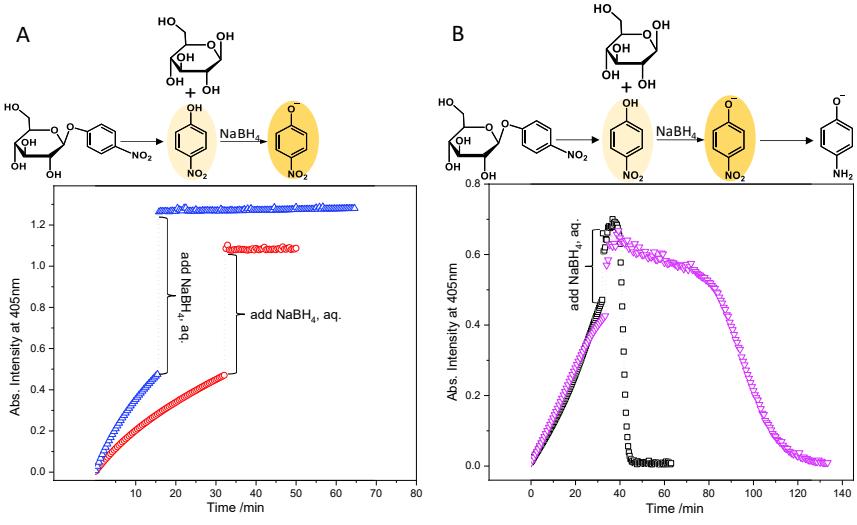

Figure 21. Cascade catalysis. A) (Δ) BG and (○) BG-PNAGA6 B) (□)Ag-BG-PNAGA6 and (▽)BG-PNAGA6 and Ag-PNAGA mixture.

In the case of Ag-BG-PNAGA6 microgels, the reduction of 4-nitrophenol by AgNPs begins shortly after the addition of $NaBH_4$, Fig. 21B. The benefit of the close proximity of the enzyme and

chemocatalyst to reaction kinetics is seen when a mixture of BG-PNAGA6 and Ag-PNAGA microgels is studied. When two catalysts were separated in different microgels, the reaction induction time was longer and it took longer time to complete.

Ag-P(NAGA-MAA) microgels

In order to compare the catalytic efficiency of the Ag-P(NAGA-MAA) microgels and the effect of AgNP preparation method, the kinetics of 4-nitrophenol reduction was studied at 30 ºC when all the microgels are in the swollen state. Chemically reduced Ag-P(NAGA) microgel exhibits similar induction time to PNAGA microgel containing UV-reduced AgNPs, Fig. 22. This is due to the similar diffusion rates that are responsible for the induction period. However, it is observed that the photocatalyzed AgNPs displays higher catalytic rate than chemically reduced AgNPs due to their smaller size and larger surface area.

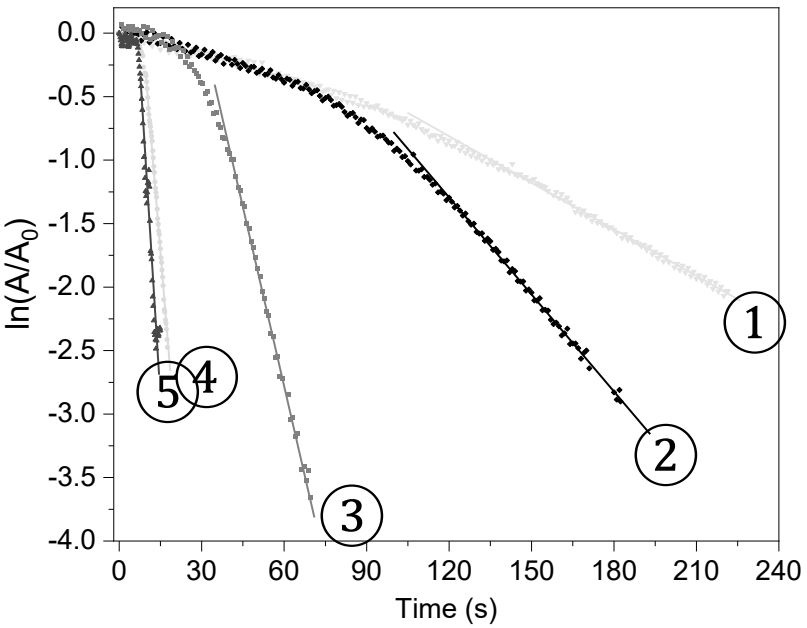

Figure 22. Kinetics of 4-NP catalysis monitored by UV. 1. Chemically reduced and 2-5 UV-reduced. 1. AgNP-PNAGA, 2. AgNP-PNAGA, 3. AgNP-P(NAGA90-MAA10), 4. AgNP-P(NAGA70-MAA30) and 5. AgNP-P(NAGA50-MAA50).

Increasing the MAA content shortens the induction time and increases the reaction rate. By incorporation of MAA units, microgel swells leading to faster diffusion and for 30 and 50% MAA-containing AgNP microgels the catalysis starts nearly immediately. Further, higher MAA content ends with higher AgNPs loading. The apparent rate constants, K_{app}, obtained from the kinetic curves were normalized to Ag mass. The Ag mass-normalized data shows that MAA content improves

catalysis efficiency of hybrid P(NAGA-MAA) microgels as smaller AgNPs have a larger surface-to-volume ratio providing more binding sites for faster catalysis.

5. Conclusions

Thermosensitive poly(N-acryloylglycinamide) (PNAGA) microgels were prepared by aqueous free radical precipitation polymerization at temperature lower than the phase transition of PNAGA. The microgels exhibit reversible swelling and shrinking upon heating and cooling in the temperature range from 5 to 70 °C. Hybrid microgels containing AgNPs were prepared by reducing $AgNO_3$ inside them. These hybrid microgels retain the thermosensitive behavior and are able to catalyse the reduction of 4-nitrophenol in the aqueous dispersion. Upon heating the catalytic efficiency of PNAGA microgels increases due to the increased diffusivity of reactants in the swollen PNAGA microgel. The thermosensitive behavior of PNAGA microgels can be utilized to control their catalytic activity by a change of temperature.

Enzyme β-D-glucosidase was encapsulated inside PNAGA microgels with different degrees of crosslinking and enzyme to polymer ratios. The enzyme encapsulated microgels also shrink upon cooling and swell upon heating. Their phase transitions can be observed calorimetrically upon heating, as the PNAGA gives a broad endothermic transition with maximum at around 45 ºC and the enzyme at 70 ºC. Compared to the free enzyme, the microgel immobilized enzymes do not aggregate at elevated temperature. Their unfolding temperatures increase and the enthalpy of the enzyme unfolding decreases. The cleavage of p-nitrophenyl-β-D-glucopyranoside, pNPG, was selected as a model to investigate the catalytic activity the enzyme immobilized microgels under different conditions. The immobilized enzymes showed activities comparable to the native enzyme at neutral and acidic pH. The hybrid microgels with higher crosslinking density shielded the enzymes and retained their catalytic activity at basic pH. Bicatalytic microgels were produced by adding AgNPs inside the enzyme containing gel particles. In the cascade reaction of enzymatic cleavage of pNPG followed by AgNP catalyzed reduction of the cleavage product 4-nitrophenol to 4-aminophenol, the hybrid microgel combining chemo- and biocatalyst performs much better than a mixture of the two catalysts residing in different microgels.

Dual thermo and pH-sensitive microgels based on P(NAGA−MAA) were prepared and their phase transition behaviour, as well as Ag nanoparticle catalyst encapsulation and catalysis efficiency were investigated. P(NAGA-MAA) microgels increase in size upon heating and show a UCST-type volume phase transition. Unlike PNAGA, the P(NAGA−MAA) copolymer microgels do not show phase transitions at neutral pH, as above the pK_a of MAA, the hydrogen bonding interactions between NAGA and MAA units are disturbed by the incorporated ionic groups. At pH 3, all copolymer microgels show a UCST-type temperature-sensitive behavior, clouding at lower temperature and clearing upon heating. However, the cloud point (Tc) showed a complex dependency on the MAA content, the Tc first decreasing upon increasing MAA up to 10 mol % and then increasing with further increasing MAA contents. DSC measurements revealed two endothermic processes occurring during the heating of P(NAGA) microgels. For copolymer microgels, the transitions occurred at lower temperatures and the enthalpies decreased with increasing MAA content. A combination of methods investigating the phase transition temperature was used to understand different aspects of the phase transition process. AgNPs were loaded inside P(NAGA-MAA) microgels by UV irradiation. The UV-reduced AgNPs are much smaller than those reduced by $NaBH_4$. The number of the AgNPs increased with increasing MAA content and at the same time, their size decreased. Catalysis tests using 4-nitrophenol reduction as a model reaction showed fastest reaction kinetics for the microgels with the highest MAA content due to the high loading and surface area of the AgNPs.

6. References

(1) Kuckling, D.; Doering, A.; Krahl, F.; Arndt, K.-F. 8.15 - Stimuli-Responsive Polymer Systems. In *Polymer Science: A Comprehensive Reference*; Matyjaszewski, K., Möller, M., Eds.; Elsevier: Amsterdam, 2012; pp 377–413. https://doi.org/10.1016/B978-0-444-53349-4.00214-4.

(2) Zhuang, J.; Gordon, M. R.; Ventura, J.; Li, L.; Thayumanavan, S. Multi-Stimuli Responsive Macromolecules and Their Assemblies. *Chem. Soc. Rev.* **2013**, *42* (17), 7421–7435. https://doi.org/10.1039/C3CS60094G.

(3) Motornov, M.; Roiter, Y.; Tokarev, I.; Minko, S. Stimuli-Responsive Nanoparticles, Nanogels and Capsules for Integrated Multifunctional Intelligent Systems. *Prog. Polym. Sci.* **2010**, *35* (1–2), 174–211. https://doi.org/10.1016/j.progpolymsci.2009.10.004.

(4) Aseyev, V.; Tenhu, H.; Winnik, F. M. Non-Ionic Thermoresponsive Polymers in Water. In *Self Organized Nanostructures of Amphiphilic Block Copolymers Ii*; Muller, A. H. E., Borisov, O., Eds.; Springer-Verlag Berlin: Berlin, 2011; Vol. 242, pp 29–89.

(5) Kim, Y.-J.; Matsunaga, Y. T. Thermo-Responsive Polymers and Their Application as Smart Biomaterials. *J. Mater. Chem. B* **2017**, *5* (23), 4307–4321. https://doi.org/10.1039/C7TB00157F.

(6) Zhu, Y.; Batchelor, R.; Lowe, A. B.; Roth, P. J. Design of Thermoresponsive Polymers with Aqueous LCST, UCST, or Both: Modification of a Reactive Poly(2-Vinyl-4,4-Dimethylazlactone) Scaffold. *Macromolecules* **2016**, *49* (2), 672–680. https://doi.org/10.1021/acs.macromol.5b02056.

(7) Liu, C.; Qin, H.; T. Mather, P. Review of Progress in Shape-Memory Polymers. *J. Mater. Chem.* **2007**, *17* (16), 1543–1558. https://doi.org/10.1039/B615954K.

(8) Soppimath, K. S.; Aminabhavi, T. M.; Dave, A. M.; Kumbar, S. G.; Rudzinski, W. E. Stimulus-Responsive "Smart" Hydrogels as Novel Drug Delivery Systems. *Drug Dev. Ind. Pharm.* **2002**, *28* (8), 957–974. https://doi.org/10.1081/DDC-120006428.

(9) Maeda, T.; Akasaki, Y.; Yamamoto, K.; Aoyagi, T. Stimuli-Responsive Coacervate Induced in Binary Functionalized Poly(N-Isopropylacrylamide) Aqueous System and Novel Method for Preparing Semi-IPN Microgel Using the Coacervate. *Langmuir* **2009**, *25* (16), 9510–9517. https://doi.org/10.1021/la9007735.

(10) Liu, R.; Fraylich, M.; Saunders, B. R. Thermoresponsive Copolymers: From Fundamental Studies to Applications. *Colloid Polym. Sci.* **2009**, *287* (6), 627–643. https://doi.org/10.1007/s00396-009-2028-x.

(11) Keerl, M.; Smirnovas, V.; Winter, R.; Richtering, W. Copolymer Microgels from Mono- and Disubstituted Acrylamides: Phase Behavior and Hydrogen Bonds. *Macromolecules* **2008**, *41* (18), 6830–6836. https://doi.org/10.1021/ma800785w.

(12) Seuring, J.; Agarwal, S. Polymers with Upper Critical Solution Temperature in Aqueous Solution. *Macromol. Rapid Commun.* **2012**, *33* (22), 1898–1920. https://doi.org/10.1002/marc.201200433.

(13) Zhu, Y.; Noy, J.-M.; Lowe, A. B.; Roth, P. J. The Synthesis and Aqueous Solution Properties of Sulfobutylbetaine (Co)Polymers: Comparison of Synthetic Routes and Tuneable Upper Critical Solution Temperatures. *Polym. Chem.* **2015**, *6* (31), 5705–5718. https://doi.org/10.1039/C5PY00160A.

(14) Yan, M.; Ge, J.; Dong, W.; Liu, Z.; Ouyang, P. Preparation and Characterization of a Temperature-Sensitive Sulfobetaine Polymer–Trypsin Conjugate. *Biochem. Eng. J.* **2006**, *30* (1), 48–54. https://doi.org/10.1016/j.bej.2006.02.001.

(15) Asadujjaman, A.; Kent, B.; Bertin, A. Phase Transition and Aggregation Behaviour of an UCST-Type Copolymer Poly(Acrylamide-Co-Acrylonitrile) in Water: Effect of Acrylonitrile Content, Concentration in Solution, Copolymer Chain Length and Presence of Electrolyte. *Soft Matter* **2017**, *13* (3), 658–669. https://doi.org/10.1039/C6SM02262F.

(16) Seuring, J.; Agarwal, S. First Example of a Universal and Cost-Effective Approach: Polymers with Tunable Upper Critical Solution Temperature in Water and Electrolyte Solution. *Macromolecules* **2012**, *45* (9), 3910–3918. https://doi.org/10.1021/ma300355k.

(17) Liu, F.; Seuring, J.; Agarwal, S. Atom Transfer Radical Polymerization as a Tool for Making Poly(N -Acryloylglycinamide) with Molar Mass Independent UCST-Type Transitions in Water and Electrolytes. *Polym. Chem.* **2013**, *4* (10), 3123–3131. https://doi.org/10.1039/C3PY00222E.

(18) Liu, F.; Seuring, J.; Agarwal, S. Controlled Radical Polymerization of N-Acryloylglycinamide and UCST-Type Phase Transition of the Polymers. *J. Polym. Sci. Part Polym. Chem.* **2012**, *50* (23), 4920–4928. https://doi.org/10.1002/pola.26322.
(19) Palanisamy, A.; Albright, V.; Sukhishvili, S. A. Upper Critical Solution Temperature Layer-by-Layer Films of Polyamino Acid-Based Micelles with Rapid, On-Demand Release Capability. *Chem. Mater.* **2017**, *29* (21), 9084–9094. https://doi.org/10.1021/acs.chemmater.7b02748.
(20) Shimada, N.; Ino, H.; Maie, K.; Nakayama, M.; Kano, A.; Maruyama, A. Ureido-Derivatized Polymers Based on Both Poly(Allylurea) and Poly(l-Citrulline) Exhibit UCST-Type Phase Transition Behavior under Physiologically Relevant Conditions. *Biomacromolecules* **2011**, *12* (10), 3418–3422. https://doi.org/10.1021/bm2010752.
(21) Xu, Z.; Liu, W. Poly(N-Acryloyl Glycinamide): A Fascinating Polymer That Exhibits a Range of Properties from UCST to High-Strength Hydrogels. *Chem. Commun.* **2018**, *54* (75), 10540–10553. https://doi.org/10.1039/C8CC04614J.
(22) Antonietti, M. Microgels. In *Encyclopedia of Materials: Science and Technology*; Buschow, K. H. J., Cahn, R. W., Flemings, M. C., Ilschner, B., Kramer, E. J., Mahajan, S., Veyssière, P., Eds.; Elsevier: Oxford, 2001; pp 5635–5636. https://doi.org/10.1016/B0-08-043152-6/00982-7.
(23) Plamper, F. A.; Richtering, W. Functional Microgels and Microgel Systems. *Acc. Chem. Res.* **2017**, *50* (2), 131–140. https://doi.org/10.1021/acs.accounts.6b00544.
(24) Baker, W. O. Microgel, a New Macromolecule. Relation to Sol and Gel as Structural Elements of Synthetic Rubber. *Rubber Chem. Technol.* **1949**, *22* (4), 935–955. https://doi.org/10.5254/1.3543023.
(25) Acciaro, R.; Gilányi, T.; Varga, I. Preparation of Monodisperse Poly(N-Isopropylacrylamide) Microgel Particles with Homogenous Cross-Link Density Distribution. *Langmuir* **2011**, *27* (12), 7917–7925. https://doi.org/10.1021/la2010387.
(26) Dai, Z.; Ngai, T. Microgel Particles: The Structure-Property Relationships and Their Biomedical Applications. *J. Polym. Sci. Part Polym. Chem.* **2013**, *51* (14), 2995–3003. https://doi.org/10.1002/pola.26698.
(27) Ren, H.; Qiu, X.-P.; Shi, Y.; Yang, P.; Winnik, F. M. The Two Phase Transitions of Hydrophobically End-Capped Poly(N-Isopropylacrylamide)s in Water. *Macromolecules* **2020**, *53* (13), 5105–5115. https://doi.org/10.1021/acs.macromol.0c00487.
(28) Gau, E.; Flecken, F.; Ksiazkiewicz, A. N.; Pich, A. Enzymatic Synthesis of Temperature-Responsive Poly(N-Vinylcaprolactam) Microgels with Glucose Oxidase. *Green Chem.* **2018**, *20* (2), 431–439. https://doi.org/10.1039/C7GC03111D.
(29) Siirilä, J.; Häkkinen, S.; Tenhu, H. The Emulsion Polymerization Induced Self-Assembly of a Thermoresponsive Polymer Poly(N -Vinylcaprolactam). *Polym. Chem.* **2019**, *10* (6), 766–775. https://doi.org/10.1039/C8PY01421C.
(30) Siirilä, J.; Hietala, S.; Ekholm, F. S.; Tenhu, H. Glucose and Maltose Surface-Functionalized Thermoresponsive Poly(N-Vinylcaprolactam) Nanogels. *Biomacromolecules* **2020**, *21* (2), 955–965. https://doi.org/10.1021/acs.biomac.9b01596.
(31) Siirilä, J.; Karesoja, M.; Pulkkinen, P.; Malho, J.-M.; Tenhu, H. Soft Poly(N-Vinylcaprolactam) Nanogels Surface-Decorated with AuNPs. Response to Temperature, Light, and RF-Field. *Eur. Polym. J.* **2019**, *115*, 59–69. https://doi.org/10.1016/j.eurpolymj.2019.03.010.
(32) Plamper, F. A.; Richtering, W. Functional Microgels and Microgel Systems. *Acc. Chem. Res.* **2017**, *50* (2), 131–140. https://doi.org/10.1021/acs.accounts.6b00544.
(33) Pich, A.; Richtering, W. Polymer Nanogels and Microgels. In *Polymer Science: A Comprehensive Reference*; Elsevier, 2012; pp 309–350. https://doi.org/10.1016/B978-0-444-53349-4.00167-9.
(34) Saunders, B. R.; Vincent, B. Microgel Particles as Model Colloids: Theory, Properties and Applications. *Adv. Colloid Interface Sci.* **1999**, *80* (1), 1–25. https://doi.org/10.1016/S0001-8686(98)00071-2.
(35) Ishii, K. Synthesis of Microgels and Their Application to Coatings. *Colloids Surf. Physicochem. Eng. Asp.* **1999**, *153* (1), 591–595. https://doi.org/10.1016/S0927-7757(98)00481-6.
(36) Pelton, R. Temperature-Sensitive Aqueous Microgels. *Adv. Colloid Interface Sci.* **2000**, *85* (1), 1–33. https://doi.org/10.1016/S0001-8686(99)00023-8.

(37) *Colloid Stability: The Role of Surface Forces*; Tadros, T. F., Ed.; Colloids and interface science series; Wiley-VCH Verlag: Weinheim, 2007.
(38) Bandyopadhyay, S.; Sharma, A.; Alvi, M. A. A.; Raju, R.; Glomm, W. R. A Robust Method to Calculate the Volume Phase Transition Temperature (VPTT) for Hydrogels and Hybrids. *RSC Adv.* **2017**, *7* (84), 53192–53202. https://doi.org/10.1039/C7RA10258E.
(39) Dušek, K.; Dušková-Smrčková, M. Volume Phase Transition in Gels: Its Discovery and Development. *Gels* **2020**, *6* (3), 22. https://doi.org/10.3390/gels6030022.
(40) Bekhradnia, S.; Zhu, K.; Knudsen, K. D.; Sande, S. A.; Nyström, B. Structure, Swelling, and Drug Release of Thermoresponsive Poly(Amidoamine) Dendrimer–Poly(N-Isopropylacrylamide) Hydrogels. *J. Mater. Sci.* **2014**, *49* (17), 6102–6110. https://doi.org/10.1007/s10853-014-8340-y.
(41) Klinger, D.; Landfester, K. Stimuli-Responsive Microgels for the Loading and Release of Functional Compounds: Fundamental Concepts and Applications. *Polymer* **2012**, *53* (23), 5209–5231. https://doi.org/10.1016/j.polymer.2012.08.053.
(42) Oh, J. K.; Drumright, R.; Siegwart, D. J.; Matyjaszewski, K. The Development of Microgels/Nanogels for Drug Delivery Applications. *Prog. Polym. Sci.* **2008**, *33* (4), 448–477. https://doi.org/10.1016/j.progpolymsci.2008.01.002.
(43) Wang, W.; Tian, X.; Feng, Y.; Cao, B.; Yang, W.; Zhang, L. Thermally On−Off Switching Membranes Prepared by Pore-Filling Poly(N-Isopropylacrylamide) Hydrogels. *Ind. Eng. Chem. Res.* **2010**, *49* (4), 1684–1690. https://doi.org/10.1021/ie9008666.
(44) Li, P.-F.; Ju, X.-J.; Chu, L.-Y.; Xie, R. Thermo-Responsive Membranes with Cross-Linked Poly(N-Isopropyl-Acrylamide) Hydrogels inside Porous Substrates. *Chem. Eng. Technol.* **2006**, *29* (11), 1333–1339. https://doi.org/10.1002/ceat.200600174.
(45) Arndt, K.-F.; Kuckling, D.; Richter, A. Application of Sensitive Hydrogels in Flow Control. *Polym. Adv. Technol.* **2000**, *11* (8–12), 496–505. https://doi.org/10.1002/1099-1581(200008/12)11:8/12<496::AID-PAT996>3.0.CO;2-7.
(46) Yu, C.; Mutlu, S.; Selvaganapathy, P.; Mastrangelo, C. H.; Svec, F.; Fréchet, J. M. J. Flow Control Valves for Analytical Microfluidic Chips without Mechanical Parts Based on Thermally Responsive Monolithic Polymers. *Anal. Chem.* **2003**, *75* (8), 1958–1961. https://doi.org/10.1021/ac026455j.
(47) Thorne, J. B.; Vine, G. J.; Snowden, M. J. Microgel Applications and Commercial Considerations. *Colloid Polym. Sci.* **2011**, *289* (5), 625. https://doi.org/10.1007/s00396-010-2369-5.
(48) Begum, R.; Naseem, K.; Farooqi, Z. H. A Review of Responsive Hybrid Microgels Fabricated with Silver Nanoparticles: Synthesis, Classification, Characterization and Applications. *J. Sol-Gel Sci. Technol.* **2016**, *77* (2), 497–515. https://doi.org/10.1007/s10971-015-3896-9.
(49) Zhang, J.; Zhang, M.; Tang, K.; Verpoort, F.; Sun, T. Polymer-Based Stimuli-Responsive Recyclable Catalytic Systems for Organic Synthesis. *Small* **2014**, *10* (1), 32–46. https://doi.org/10.1002/smll.201300287.
(50) Mizrahi, B.; Irusta, S.; McKenna, M.; Stefanescu, C.; Yedidsion, L.; Myint, M.; Langer, R.; Kohane, D. S. Microgels for Efficient Protein Purification. *Adv. Mater.* **2011**, *23* (36), H258–H262. https://doi.org/10.1002/adma.201101258.
(51) Su, S.; Ali, Md. M.; Filipe, C. D. M.; Li, Y.; Pelton, R. Microgel-Based Inks for Paper-Supported Biosensing Applications. *Biomacromolecules* **2008**, *9* (3), 935–941. https://doi.org/10.1021/bm7013608.
(52) Toma, M.; Jonas, U.; Mateescu, A.; Knoll, W.; Dostalek, J. Active Control of SPR by Thermoresponsive Hydrogels for Biosensor Applications. *J. Phys. Chem. C* **2013**, *117* (22), 11705–11712. https://doi.org/10.1021/jp400255u.
(53) Islam, M. R.; Ahiabu, A.; Li, X.; Serpe, M. J. Poly (N-Isopropylacrylamide) Microgel-Based Optical Devices for Sensing and Biosensing. *Sensors* **2014**, *14* (5), 8984–8995. https://doi.org/10.3390/s140508984.
(54) Wu, X.; Pelton, R. H.; Hamielec, A. E.; Woods, D. R.; McPhee, W. The Kinetics of Poly(N-Isopropylacrylamide) Microgel Latex Formation. *Colloid Polym. Sci.* **1994**, *272* (4), 467–477. https://doi.org/10.1007/BF00659460.

(55) Lee, H.; Mok, H.; Lee, S.; Oh, Y.-K.; Park, T. G. Target-Specific Intracellular Delivery of SiRNA Using Degradable Hyaluronic Acid Nanogels. *J. Controlled Release* **2007**, *119* (2), 245–252. https://doi.org/10.1016/j.jconrel.2007.02.011.
(56) Jha, A. K.; Hule, R. A.; Jiao, T.; Teller, S. S.; Clifton, R. J.; Duncan, R. L.; Pochan, D. J.; Jia, X. Structural Analysis and Mechanical Characterization of Hyaluronic Acid-Based Doubly Cross-Linked Networks. *Macromolecules* **2009**, *42* (2), 537–546. https://doi.org/10.1021/ma8019442.
(57) Gan, D.; Lyon, L. A. Synthesis and Protein Adsorption Resistance of PEG-Modified Poly(N-Isopropylacrylamide) Core/Shell Microgels. *Macromolecules* **2002**, *35* (26), 9634–9639. https://doi.org/10.1021/ma021186k.
(58) Wolff, H. J. M.; Kather, M.; Breisig, H.; Richtering, W.; Pich, A.; Wessling, M. From Batch to Continuous Precipitation Polymerization of Thermoresponsive Microgels. *ACS Appl. Mater. Interfaces* **2018**, *10* (29), 24799–24806. https://doi.org/10.1021/acsami.8b06920.
(59) Hu, X.; Tong, Z.; Lyon, L. A. Control of Poly(N-Isopropylacrylamide) Microgel Network Structure by Precipitation Polymerization near the Lower Critical Solution Temperature. *Langmuir* **2011**, *27* (7), 4142–4148. https://doi.org/10.1021/la200114s.
(60) Wang, Y.; Nie, J.; Chang, B.; Sun, Y.; Yang, W. Poly(Vinylcaprolactam)-Based Biodegradable Multiresponsive Microgels for Drug Delivery. *Biomacromolecules* **2013**, *14* (9), 3034–3046. https://doi.org/10.1021/bm401131w.
(61) Janssen, F. A. L.; Kather, M.; Kröger, L. C.; Mhamdi, A.; Leonhard, K.; Pich, A.; Mitsos, A. Synthesis of Poly(N-Vinylcaprolactam)-Based Microgels by Precipitation Polymerization: Process Modeling and Experimental Validation. *Ind. Eng. Chem. Res.* **2017**, *56* (49), 14545–14556. https://doi.org/10.1021/acs.iecr.7b03263.
(62) Pich, A.; Richtering, W. Microgels by Precipitation Polymerization: Synthesis, Characterization, and Functionalization. In *Chemical Design of Responsive Microgels*; Pich, A., Richtering, W., Eds.; Advances in Polymer Science; Springer: Berlin, Heidelberg, 2011; pp 1–37. https://doi.org/10.1007/12_2010_70.
(63) Kratz, K.; Lapp, A.; Eimer, W.; Hellweg, T. Volume Transition and Structure of Triethyleneglycol Dimethacrylate, Ethylenglykol Dimethacrylate, and N,N'-Methylene Bis-Acrylamide Cross-Linked Poly(N-Isopropyl Acrylamide) Microgels: A Small Angle Neutron and Dynamic Light Scattering Study. *Colloids Surf. Physicochem. Eng. Asp.* **2002**, *197* (1), 55–67. https://doi.org/10.1016/S0927-7757(01)00821-4.
(64) Panayiotou, M.; Pöhner, C.; Vandevyver, C.; Wandrey, C.; Hilbrig, F.; Freitag, R. Synthesis and Characterisation of Thermo-Responsive Poly(N,N'-Diethylacrylamide) Microgels. *React. Funct. Polym.* **2007**, *67* (9), 807–819. https://doi.org/10.1016/j.reactfunctpolym.2006.12.008.
(65) Pich, A.; Berger, S.; Ornatsky, O.; Baranov, V.; Winnik, M. A. The Influence of PEG Macromonomers on the Size and Properties of Thermosensitive Aqueous Microgels. *Colloid Polym. Sci.* **2009**, *287* (3), 269–275. https://doi.org/10.1007/s00396-008-1972-1.
(66) Fernandez, V. V. A.; Tepale, N.; Sánchez-Díaz, J. C.; Mendizábal, E.; Puig, J. E.; Soltero, J. F. A. Thermoresponsive Nanostructured Poly(N-Isopropylacrylamide) Hydrogels Made via Inverse Microemulsion Polymerization. *Colloid Polym. Sci.* **2006**, *284* (4), 387–395. https://doi.org/10.1007/s00396-005-1395-1.
(67) Braun, O.; Selb, J.; Candau, F. Synthesis in Microemulsion and Characterization of Stimuli-Responsive Polyelectrolytes and Polyampholytes Based on N-Isopropylacrylamide. *Polymer* **2001**, *42* (21), 8499–8510. https://doi.org/10.1016/S0032-3861(01)00445-1.
(68) Dowding, P. J.; Goodwin, J. W.; Vincent, B. Production of Porous Suspension Polymer Beads with a Narrow Size Distribution Using a Cross-Flow Membrane and a Continuous Tubular Reactor. *Colloids Surf. Physicochem. Eng. Asp.* **2001**, *180* (3), 301–309. https://doi.org/10.1016/S0927-7757(00)00777-9.
(69) Qi, G.; Jones, C. W.; Schork, F. J. RAFT Inverse Miniemulsion Polymerization of Acrylamide. *Macromol. Rapid Commun.* **2007**, *28* (9), 1010–1016. https://doi.org/10.1002/marc.200700026.
(70) Monteiro, M. J.; Cunningham, M. F. Polymer Colloids: Synthesis Fundamentals to Applications. *Biomacromolecules* **2020**, *21* (11), 4377–4378. https://doi.org/10.1021/acs.biomac.0c01462.

(71) Hennink, W. E.; van Nostrum, C. F. Novel Crosslinking Methods to Design Hydrogels. *Adv. Drug Deliv. Rev.* **2012**, *64*, 223–236. https://doi.org/10.1016/j.addr.2012.09.009.
(72) Van Tomme, S. R.; Storm, G.; Hennink, W. E. In Situ Gelling Hydrogels for Pharmaceutical and Biomedical Applications. *Int. J. Pharm.* **2008**, *355* (1), 1–18. https://doi.org/10.1016/j.ijpharm.2008.01.057.
(73) Hoare, T. R.; Kohane, D. S. Hydrogels in Drug Delivery: Progress and Challenges. *Polymer* **2008**, *49* (8), 1993–2007. https://doi.org/10.1016/j.polymer.2008.01.027.
(74) Hoffman, A. S. Hydrogels for Biomedical Applications. *Adv. Drug Deliv. Rev.* **2002**, *54* (1), 3–12. https://doi.org/10.1016/S0169-409X(01)00239-3.
(75) Coviello, T.; Matricardi, P.; Marianecci, C.; Alhaique, F. Polysaccharide Hydrogels for Modified Release Formulations. *J. Controlled Release* **2007**, *119* (1), 5–24. https://doi.org/10.1016/j.jconrel.2007.01.004.
(76) Lee, K. Y.; Mooney, D. J. Hydrogels for Tissue Engineering. *Chem. Rev.* **2001**, *101* (7), 1869–1880. https://doi.org/10.1021/cr000108x.
(77) Bernkop-Schnürch, A.; Schwarz, V.; Steininger, S. Polymers with Thiol Groups: A New Generation of Mucoadhesive Polymers? *Pharm. Res.* **1999**, *16* (6), 876–881. https://doi.org/10.1023/A:1018830204170.
(78) Bernkop-Schnürch, A.; Hornof, M.; Zoidl, T. Thiolated Polymers—Thiomers: Synthesis and in Vitro Evaluation of Chitosan–2-Iminothiolane Conjugates. *Int. J. Pharm.* **2003**, *260* (2), 229–237. https://doi.org/10.1016/S0378-5173(03)00271-0.
(79) Bernkop-Schnürch, A.; Guggi, D.; Pinter, Y. Thiolated Chitosans: Development and in Vitro Evaluation of a Mucoadhesive, Permeation Enhancing Oral Drug Delivery System. *J. Controlled Release* **2004**, *94* (1), 177–186. https://doi.org/10.1016/j.jconrel.2003.10.005.
(80) Loretz, B.; Thaler, M.; Bernkop-Schnürch, A. Role of Sulfhydryl Groups in Transfection? A Case Study with Chitosan−NAC Nanoparticles. *Bioconjug. Chem.* **2007**, *18* (4), 1028–1035. https://doi.org/10.1021/bc0603079.
(81) Shu, S.; Wang, X.; Zhang, X.; Zhang, X.; Wang, Z.; Li, C. Disulfide Cross-Linked Biodegradable Polyelectrolyte Nanoparticles for the Oral Delivery of Protein Drugs. *New J. Chem.* **2009**, *33* (9), 1882–1887. https://doi.org/10.1039/B903208H.
(82) Lee, H.; Jeong, Y.; Park, T. G. Shell Cross-Linked Hyaluronic Acid/Polylysine Layer-by-Layer Polyelectrolyte Microcapsules Prepared by Removal of Reducible Hyaluronic Acid Microgel Cores. *Biomacromolecules* **2007**, *8* (12), 3705–3711. https://doi.org/10.1021/bm700854j.
(83) Bae, K. H.; Mok, H.; Park, T. G. Synthesis, Characterization, and Intracellular Delivery of Reducible Heparin Nanogels for Apoptotic Cell Death. *Biomaterials* **2008**, *29* (23), 3376–3383. https://doi.org/10.1016/j.biomaterials.2008.04.035.
(84) Nichols, M. D.; Scott, E. A.; Elbert, D. L. Factors Affecting Size and Swelling of Poly(Ethylene Glycol) Microspheres Formed in Aqueous Sodium Sulfate Solutions without Surfactants. *Biomaterials* **2009**, *30* (29), 5283–5291. https://doi.org/10.1016/j.biomaterials.2009.06.032.
(85) Scott, E. A.; Nichols, M. D.; Cordova, L. H.; George, B. J.; Jun, Y.-S.; Elbert, D. L. Protein Adsorption and Cell Adhesion on Nanoscale Bioactive Coatings Formed from Poly(Ethylene Glycol) and Albumin Microgels. *Biomaterials* **2008**, *29* (34), 4481–4493. https://doi.org/10.1016/j.biomaterials.2008.08.003.
(86) Can, M.; Sahiner, N. A Facile One-Pot Synthesis of Microgels and Nanogels of Laminarin for Biomedical Applications. *J. Colloid Interface Sci.* **2021**, *588*, 40–49. https://doi.org/10.1016/j.jcis.2020.12.053.
(87) Hoare, T.; Pelton, R. Charge-Switching, Amphoteric Glucose-Responsive Microgels with Physiological Swelling Activity. *Biomacromolecules* **2008**, *9* (2), 733–740. https://doi.org/10.1021/bm701203r.
(88) Letchford, K.; Burt, H. A Review of the Formation and Classification of Amphiphilic Block Copolymer Nanoparticulate Structures: Micelles, Nanospheres, Nanocapsules and Polymersomes. *Eur. J. Pharm. Biopharm.* **2007**, *65* (3), 259–269. https://doi.org/10.1016/j.ejpb.2006.11.009.
(89) Cho, H. K.; Cheong, I. W.; Lee, J. M.; Kim, J. H. Polymeric Nanoparticles, Micelles and Polymersomes from Amphiphilic Block Copolymer. *Korean J. Chem. Eng.* **2010**, *27* (3), 731–740. https://doi.org/10.1007/s11814-010-0216-5.

(90) Li, H.; Mergel, O.; Jain, P.; Li, X.; Peng, H.; Rahimi, K.; Singh, S.; A. Plamper, F.; Pich, A. Electroactive and Degradable Supramolecular Microgels. *Soft Matter* **2019**, *15* (42), 8589–8602. https://doi.org/10.1039/C9SM01390C.
(91) Newsom, J. P.; Payne, K. A.; Krebs, M. D. Microgels: Modular, Tunable Constructs for Tissue Regeneration. *Acta Biomater.* **2019**, *88*, 32–41. https://doi.org/10.1016/j.actbio.2019.02.011.
(92) Lu, Y.; Proch, S.; Schrinner, M.; Drechsler, M.; Kempe, R.; Ballauff, M. Thermosensitive Core-Shell Microgel as a "Nanoreactor" for Catalytic Active Metal Nanoparticles. *J. Mater. Chem.* **2009**, *19* (23), 3955–3961. https://doi.org/10.1039/B822673N.
(93) Lu, Y.; Mei, Y.; Ballauff, M.; Drechsler, M. Thermosensitive Core−Shell Particles as Carrier Systems for Metallic Nanoparticles. *J. Phys. Chem. B* **2006**, *110* (9), 3930–3937. https://doi.org/10.1021/jp057149n.
(94) Thomas, V.; Namdeo, M.; Mohan, Y. M.; Bajpai, S. K.; Bajpai, M. Review on Polymer, Hydrogel and Microgel Metal Nanocomposites: A Facile Nanotechnological Approach. *J. Macromol. Sci. Part A* **2007**, *45* (1), 107–119. https://doi.org/10.1080/10601320701683470.
(95) Lu, Y.; Mei, Y.; Drechsler, M.; Ballauff, M. Thermosensitive Core–Shell Particles as Carriers for Ag Nanoparticles: Modulating the Catalytic Activity by a Phase Transition in Networks. *Angew. Chem. Int. Ed.* **2006**, *45* (5), 813–816. https://doi.org/10.1002/anie.200502731.
(96) Schrinner, M.; Proch, S.; Mei, Y.; Kempe, R.; Miyajima, N.; Ballauff, M. Stable Bimetallic Gold–Platinum Nanoparticles Immobilized on Spherical Polyelectrolyte Brushes: Synthesis, Characterization, and Application for the Oxidation of Alcohols. *Adv. Mater.* **2008**, *20* (10), 1928–1933. https://doi.org/10.1002/adma.200702421.
(97) Biffis, A.; Cunial, S.; Spontoni, P.; Prati, L. Microgel-Stabilized Gold Nanoclusters: Powerful "Quasi-Homogeneous" Catalysts for the Aerobic Oxidation of Alcohols in Water. *J. Catal.* **2007**, *251* (1), 1–6. https://doi.org/10.1016/j.jcat.2007.07.024.
(98) Khan, A.; El-Toni, A. M.; Alrokayan, S.; Alsalhi, M.; Alhoshan, M.; Aldwayyan, A. S. Microwave-Assisted Synthesis of Silver Nanoparticles Using Poly-N-Isopropylacrylamide/Acrylic Acid Microgel Particles. *Colloids Surf. Physicochem. Eng. Asp.* **2011**, *377* (1), 356–360. https://doi.org/10.1016/j.colsurfa.2011.01.042.
(99) Zdarta, J.; Meyer, A. S.; Jesionowski, T.; Pinelo, M. A General Overview of Support Materials for Enzyme Immobilization: Characteristics, Properties, Practical Utility. *Catalysts* **2018**, *8* (2), 92. https://doi.org/10.3390/catal8020092.
(100) Lancaster, L.; Abdallah, W.; Banta, S.; Wheeldon, I. Engineering Enzyme Microenvironments for Enhanced Biocatalysis. *Chem. Soc. Rev.* **2018**, *47* (14), 5177–5186. https://doi.org/10.1039/C8CS00085A.
(101) Sheldon, R. A. Engineering a More Sustainable World through Catalysis and Green Chemistry. *J. R. Soc. Interface* **2016**, *13* (116), 20160087. https://doi.org/10.1098/rsif.2016.0087.
(102) Sheldon, R. A.; Pelt, S. van. Enzyme Immobilisation in Biocatalysis: Why, What and How. *Chem. Soc. Rev.* **2013**, *42* (15), 6223–6235. https://doi.org/10.1039/C3CS60075K.
(103) Yan, M.; Ge, J.; Liu, Z.; Ouyang, P. Encapsulation of Single Enzyme in Nanogel with Enhanced Biocatalytic Activity and Stability. *J. Am. Chem. Soc.* **2006**, *128* (34), 11008–11009. https://doi.org/10.1021/ja064126t.
(104) Beloqui, A.; Kobitski, A. Y.; Nienhaus, G. U.; Delaittre, G. A Simple Route to Highly Active Single-Enzyme Nanogels. *Chem. Sci.* **2018**, *9* (4), 1006–1013. https://doi.org/10.1039/C7SC04438K.
(105) Haas, H. C.; Schuler, N. W. Thermally Reversible Homopolymer Gel Systems. *J. Polym. Sci. [B]* **1964**, *2* (12), 1095–1096. https://doi.org/10.1002/pol.1964.110021203.
(106) Haas, H. C.; Moreau, R. D.; Schuler, N. W. Synthetic Thermally Reversible Gel Systems. II. *J. Polym. Sci. Part -2 Polym. Phys.* **1967**, *5* (5), 915–927. https://doi.org/10.1002/pol.1967.160050509.
(107) Marstokk, O.; Nyström, B.; Roots, J. Effect of Denaturant and Polymer Concentration on the Structural and Dynamical Properties of Aqueous Solutions of Poly(N-Acetamido Acrylamide). *Macromolecules* **1998**, *31* (13), 4205–4212. https://doi.org/10.1021/ma980049d.

(108) Seuring, J.; Bayer, F. M.; Huber, K.; Agarwal, S. Upper Critical Solution Temperature of Poly(N-Acryloyl Glycinamide) in Water: A Concealed Property. *Macromolecules* **2012**, *45* (1), 374–384. https://doi.org/10.1021/ma202059t.

(109) Matyjaszewski, K.; Xia, J. Atom Transfer Radical Polymerization. *Chem. Rev.* **2001**, *101* (9), 2921–2990. https://doi.org/10.1021/cr940534g.

(110) Tang, Y.; Wu, T.; Hu, B.; Yang, Q.; Liu, L.; Yu, B.; Ding, Y.; Ye, S. Synthesis of Thermo- and PH-Responsive Ag Nanoparticle-Embedded Hybrid Microgels and Their Catalytic Activity in Methylene Blue Reduction. *Mater. Chem. Phys.* **2015**, *149–150*, 460–466. https://doi.org/10.1016/j.matchemphys.2014.10.045.

(111) Sun, W.; An, Z.; Wu, P. Hydrogen Bonding Reinforcement as a Strategy to Improve Upper Critical Solution Temperature of Poly(N-Acryloylglycinamide-Co-Methacrylic Acid). *Polym. Chem.* **2018**, *9* (26), 3667–3673. https://doi.org/10.1039/C8PY00733K.

(112) Slistan-Grijalva, A.; Herrera-Urbina, R.; Rivas-Silva, J. F.; Ávalos-Borja, M.; Castillón-Barraza, F. F.; Posada-Amarillas, A. Classical Theoretical Characterization of the Surface Plasmon Absorption Band for Silver Spherical Nanoparticles Suspended in Water and Ethylene Glycol. *Phys. E Low-Dimens. Syst. Nanostructures* **2005**, *27* (1), 104–112. https://doi.org/10.1016/j.physe.2004.10.014.

(113) Zhang, J.; Xu, S.; Kumacheva, E. Photogeneration of Fluorescent Silver Nanoclusters in Polymer Microgels. *Adv. Mater.* **2005**, *17* (19), 2336–2340. https://doi.org/10.1002/adma.200501062.

(114) Liu, F.; Seuring, J.; Agarwal, S. A Non-Ionic Thermophilic Hydrogel with Positive Thermosensitivity in Water and Electrolyte Solution. *Macromol. Chem. Phys.* **2014**, *215* (15), 1466–1472. https://doi.org/10.1002/macp.201400155.

(115) Guillermo, A.; Addad, J. P. C.; Bazile, J. P.; Duracher, D.; Elaissari, A.; Pichot, C. NMR Investigations into Heterogeneous Structures of Thermosensitive Microgel Particles. *J. Polym. Sci. Part B Polym. Phys.* **2000**, *38* (6), 889–898. https://doi.org/10.1002/(SICI)1099-0488(20000315)38:6<889::AID-POLB9>3.0.CO;2-L.

(116) Obeid, R.; Tanaka, F.; Winnik, F. M. Heat-Induced Phase Transition and Crystallization of Hydrophobically End-Capped Poly(2-Isopropyl-2-Oxazoline)s in Water. *Macromolecules* **2009**, *42* (15), 5818–5828. https://doi.org/10.1021/ma900838v.

(117) Ballauff, M.; Lu, Y. "Smart" Nanoparticles: Preparation, Characterization and Applications. *Polymer* **2007**, *48* (7), 1815–1823. https://doi.org/10.1016/j.polymer.2007.02.004.

(118) Liu, Y.-Y.; Liu, X.-Y.; Yang, J.-M.; Lin, D.-L.; Chen, X.; Zha, L.-S. Investigation of Ag Nanoparticles Loading Temperature Responsive Hybrid Microgels and Their Temperature Controlled Catalytic Activity. *Colloids Surf. Physicochem. Eng. Asp.* **2012**, *393*, 105–110. https://doi.org/10.1016/j.colsurfa.2011.11.007.

(119) Woodward, J.; Wiseman, A. Fungal and Other β-d-Glucosidases — Their Properties and Applications. *Enzyme Microb. Technol.* **1982**, *4* (2), 73–79. https://doi.org/10.1016/0141-0229(82)90084-9.